nature metabolism

Letter

https://doi.org/10.1038/s42255-024-01153-1

Skeletal muscle from *TBC1D4* p.Arg684Ter variant carriers is severely insulin resistant but exhibits normal metabolic responses during exercise

Received: 3 November 2023

Accepted: 27 September 2024

Published online: 31 October 2024

Check for updates

A list of authors and their affiliations appears at the end of the paper

In the Greenlandic Inuit population, 4% are homozygous carriers of a genetic nonsense *TBC1D4* p.Arg684Ter variant leading to loss of the muscle-specific isoform of TBC1D4 and an approximately tenfold increased risk of type 2 diabetes[1]. Here we show the metabolic consequences of this variant in four female and four male homozygous carriers and matched controls. An extended glucose tolerance test reveals prolonged hyperglycaemia followed by reactive hypoglycaemia in the carriers. Whole-body glucose disposal is impaired during euglycaemic-hyperinsulinaemic clamp conditions and associates with severe insulin resistance in skeletal muscle only. Notably, a marked reduction in muscle glucose transporter GLUT4 and associated proteins is observed. While metabolic regulation during exercise remains normal, the insulin-sensitizing effect of a single exercise bout is compromised. Thus, loss of the muscle-specific isoform of TBC1D4 causes severe skeletal muscle insulin resistance without baseline hyperinsulinaemia. However, physical activity can ameliorate this condition. These observations offer avenues for personalized interventions and targeted preventive strategies.

The prevalence of obesity and type 2 diabetes (T2D) in the indigenous Arctic Inuit populations is increasing rapidly[2]. Interactions between genetics and lifestyle behaviour for the risk of developing T2D during the transition from a traditional hunter–gatherer lifestyle to a modern industrialized lifestyle have been incompletely studied[3–5]. Previously, we found a common genetic nonsense *TBC1D4* p.Arg684Ter variant with an allele frequency of 17% in the Greenlandic Inuit population[1]. Homozygous carriers of this variant have impaired glucose tolerance and an approximately tenfold increased risk of T2D, and the p.Arg684Ter variant explains approximately 10% of T2D occurrence in the Greenlandic Inuit population surveys[1]. The p.Arg684Ter variant causes a premature stop codon in the long isoform of *TBC1D4*, which is expressed almost exclusively in skeletal and cardiac muscle. The stop variant is not present in the short isoform of *TBC1D4*, and in the carriers, the expression of this isoform is normal in organs such as the pancreas, adipose tissue and liver[1]. Thus, homozygous carriers of the p.Arg684Ter variant can be considered a human quasi-muscle-specific TBC1D4-deficient model.

The metabolic and molecular consequences of lacking TBC1D4 in human skeletal muscle, and how this leads to glucose intolerance remain unsolved. Preclinical studies suggest that TBC1D4 regulates glucose transport via translocation of glucose transporter 4 (GLUT4) storage vesicles to the plasma membrane[6–8]. Notably, phospho-regulation of TBC1D4 in skeletal muscle is impaired in insulin resistant participants and patients with T2D (refs. 9–12), and improvement of insulin sensitivity following exercise training[11] and pioglitazone treatment[10] is accompanied by normalization of TBC1D4 phosphorylation. These observations suggest that signalling through TBC1D4 is important for insulin action and is modulated by exercise.

e-mail: jw@nexs.ku.dk

https://doi.org/10.1038/s42255-024-01153-1

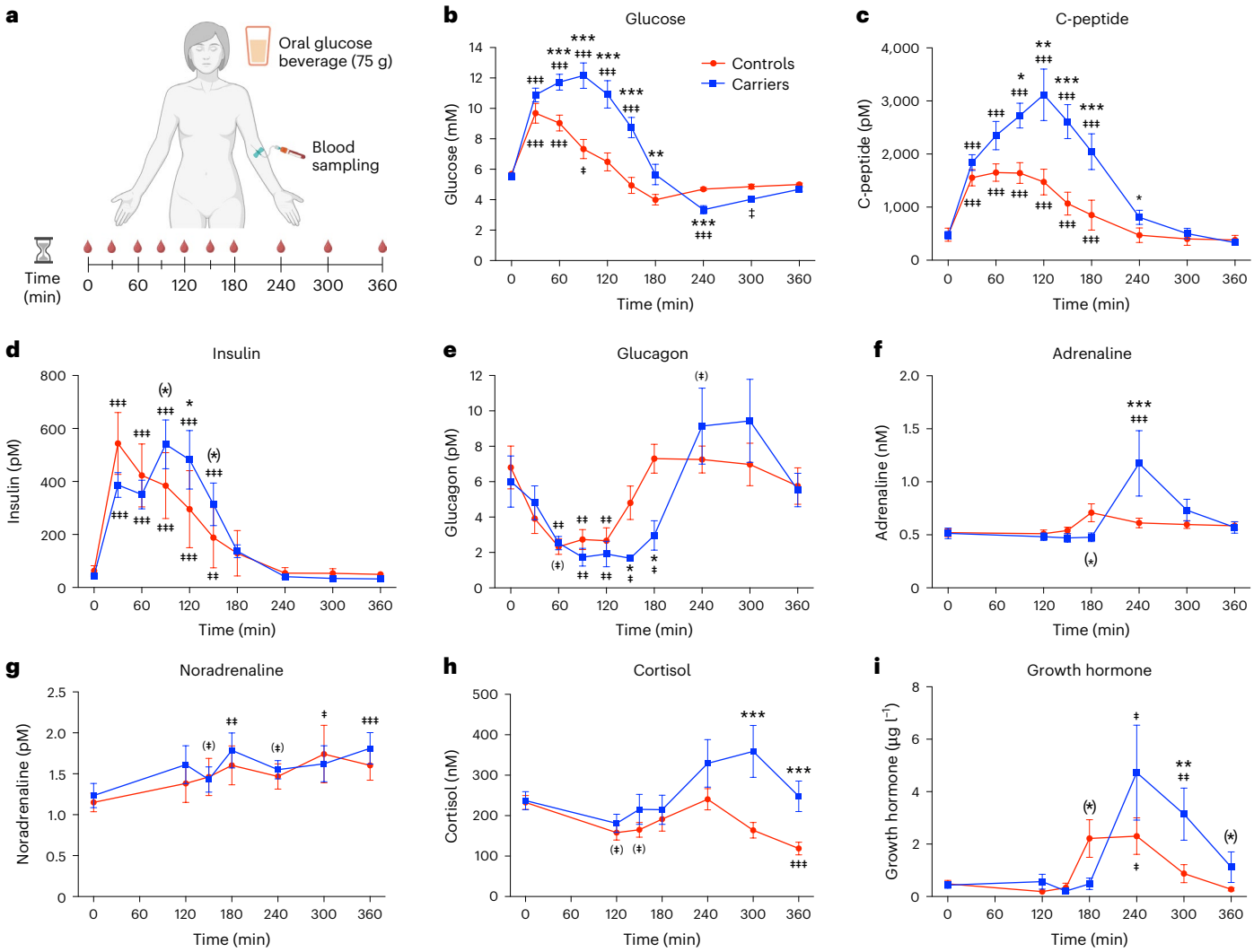

Fig. 1 | Homozygous *TBC1D4* p.Arg684Ter variant carriers display prolonged hyperglycaemia followed by hypoglycaemia during an extended oral glucose challenge. a, Graphical representation of the OGTT. **b**–**i**, Blood glucose (**b**) as well as plasma C-peptide (**c**), insulin (**d**), glucagon (**e**), adrenaline (**f**), noradrenaline (**g**), cortisol (**h**) and growth hormone (**i**) during an extended (6 h) OGTT. *Difference between TBC1D4 carriers and Controls at the given time point. ‡Different from basal (time 0) within the same group. One symbol $P < 0.05$. Two symbols $P < 0.01$. Three symbols $P < 0.001$. Symbols within parentheses represent P values between 0.1 and 0.05. $n = 8$ in Controls and $n = 7$ in TBC1D4 carriers. Data are means ± s.e.m. Data were analysed using a two-way repeated ANOVA test (one factor repeated) and two-tailed Student–Newman–Keuls post hoc analyses for multiple comparisons. Graphics in **a** created using BioRender.com.

The study of the Greenlandic carriers of the *TBC1D4* p.Arg684Ter variant provides a unique opportunity to explore the putative causal link between TBC1D4 and the ability of insulin and exercise to regulate muscle metabolism in humans, and importantly delineate the necessity of TBC1D4 for the insulin-sensitizing effect of exercise. Here, we provide substantial explanatory clues to the increased insulin resistance and frequency of T2D in the carriers.

In Greenland, we successfully recruited homozygous *TBC1D4* p.Arg684Ter variant carriers and a Greenlandic control group matched according to age, sex, European genetic admixture, body mass index (BMI) and physical fitness level (Extended Data Table 1). The normal fasting blood glucose, and plasma lipid levels and the pronounced glucose intolerance in the carriers, reflect what we have reported previously in a larger population survey in Greenland[1]. Here, we also report a similar body composition and total skeletal muscle mass in the carriers and controls (Extended Data Table 1).

An extended 6-hour oral glucose tolerance test (OGTT) revealed similar peak plasma glucose concentrations (~10 mM at 30 min) but prolonged hyperglycaemia (until 180 min) concomitant with elevated plasma insulin and C-peptide concentrations in the carriers (Fig. 1a–d). Thus, the carriers were severely glucose intolerant and insulin resistant. Fasting plasma incretin concentrations (Glucagon-like peptide 1 (GLP-1) and Glucose-dependent insulinotropic polypeptide (GIP)) and the incretin response during the glucose challenge was normal in the carriers (Extended Data Fig. 1a,b). The prolonged period of hyperglycaemia was followed by reactive hypoglycaemia in the carriers (~3.3 mM at 240 min) (Fig. 1b). This uncommon observation[13–15] was not caused by dysregulation of the counter-regulatory hormone response (Fig. 1e–i). We propose that the observed hypoglycaemia following an oral glucose load is caused by a combination of elevated insulin levels, and intact adipose tissue and in particular liver insulin sensitivity in the carriers (see text below). It is essential to highlight that hypoglycaemia is a recognized side effect of insulin treatment in diabetes. Even non-severe hypoglycaemia episodes are associated with an increased risk of severe hypoglycaemia and adverse cardiovascular outcomes[16]. Carriers have an increased risk of ischaemic heart disease and cardiovascular disease death, although not statistically significant[17]. Thus, the avoidance of such non-severe hypoglycaemia episodes in carriers is recommended.

https://doi.org/10.1038/s42255-024-01153-1

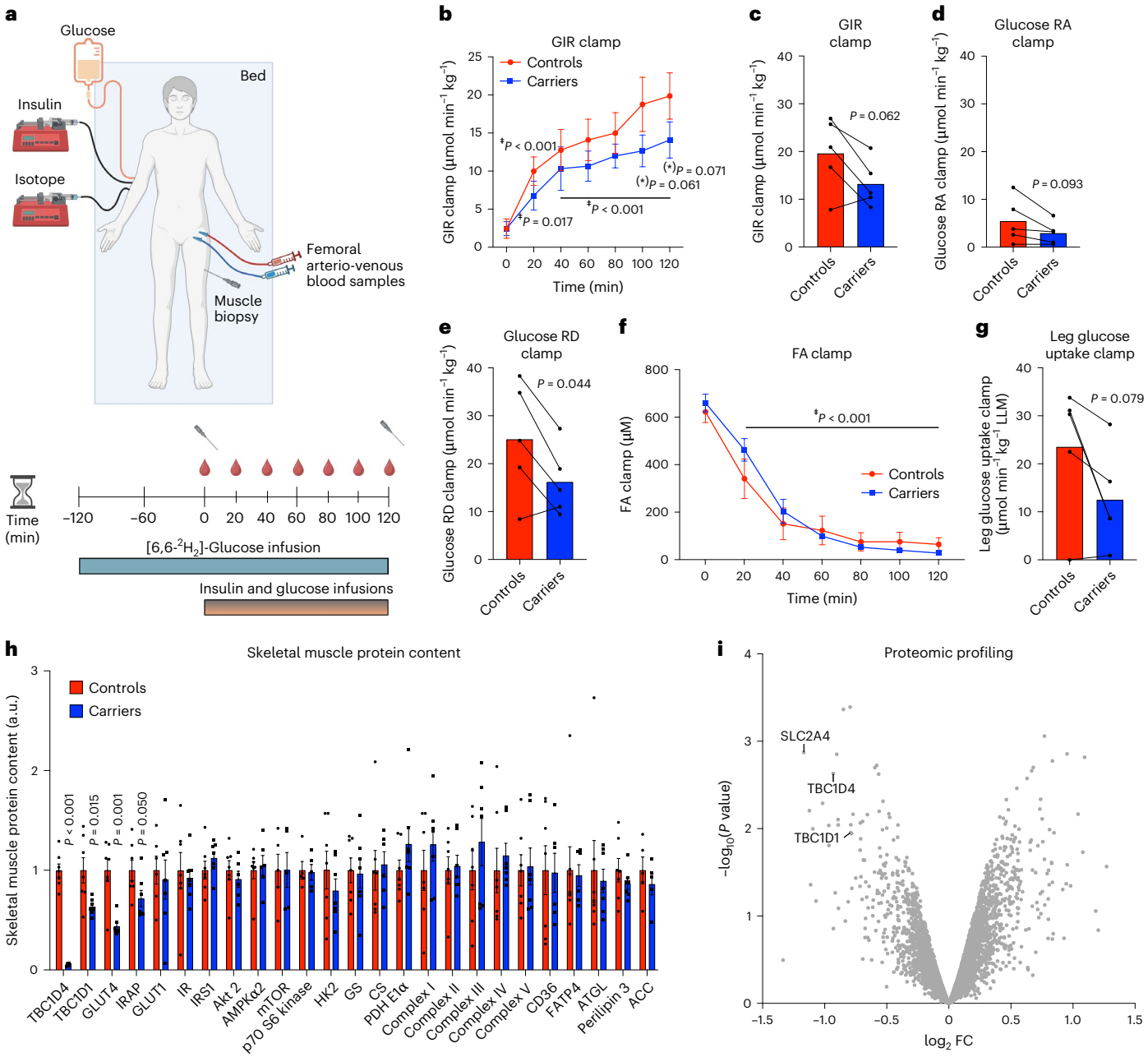

Fig. 2 | Compromised peripheral glucose disposal during EHC conditions but normal liver and adipose tissue regulation in homozygous *TBC1D4* p.Arg684Ter variant carriers. a, Graphical representation of the EHC. **b**, GIR during the insulin clamp. **c**–**e**, GIR (**c**), endogenous glucose rate of appearance (RA) (**d**) and glucose rate of disappearance (RD) (**e**) at 120 min of the clamp. **f**, Plasma FAs during the clamp. **g**, Average leg glucose uptake during the last 40 min of the clamp. **h**, Targeted immunoblotting analyses of proteins associated with glucose metabolism, fat metabolism and the mitochondrial electron transport chain in skeletal muscle. **i**, Volcano plot showing proteome $\log_2$ fold change (FC) (carriers/controls) plotted against $-\log_{10} P$ value highlighting downregulated proteins TBC1D4, TBC1D1 and GLUT4 (SLC2A4). *Difference between TBC1D4 carriers and controls at the given time point. ‡Different from basal (time 0) within the same group. $n = 5$ (**b**–**g**, **i**). $n = 7$ (**h**) except for mTOR, p70S6K and ACC ($n = 5$ in controls and TBC1D4 carriers) as well as Akt2, AMPKα2, CS, CD36 and FATP4 ($n = 6$) in controls and GLUT1 ($n = 6$) in TBC1D4 carriers. Data are means ± s.e.m. Data were analysed using a two-tailed paired Student's *t*-test (**c**–**e**, **g**), a two-tailed non-paired Student's *t*-test (**h**) as well as a two-way repeated ANOVA test (two-factor repeated) and two-tailed Student–Newman–Keuls post hoc analyses for multiple comparisons (**b**, **f**). Graphics in **a** created using BioRender.com. a.u., arbitrary units.

Five carriers and individually paired controls travelled from Greenland to our research facilities in Copenhagen for further investigations (Extended Data Table 2). The euglycaemic-hyperinsulinaemic clamp (EHC) technique was applied to evaluate whole-body insulin sensitivity (Fig. 2a). In the fasted state immediately before the clamp, endogenous glucose production as well as blood glucose and plasma insulin concentrations were similar in the carriers and controls (Extended Data Fig. 2a–c). This suggests that carriers display intact glycaemic control in the fasted state. To maintain euglycaemia during insulin stimulation, glucose infusion was increased in both groups but at the end of the EHC (120 min), glucose infusion rate (GIR) was on average ~30% lower in the carriers (Fig. 2b,c). Endogenous glucose production during insulin stimulation was similar in the carriers and controls (Fig. 2d). As a result, the glucose disappearance rate (Rd) was reduced

by ~35%, clearly demonstrating whole-body insulin resistance in the carriers (Fig. 2e). The adipose tissue insulin-resistance index during fasting (Extended Data Table 1), the insulin-mediated plasma fatty acid (FA) suppression during the EHC (Fig. 2f) and during the initial period of the OGTT (Extended Data Fig. 2d), as well as the regulation of genes in adipose tissue related to 'insulin signalling' and 'type 2 diabetes' during the EHC (Extended Data Fig. 2e and Supplementary Table 1), were similar in the carriers and controls. The insertion of catheters into both femoral veins and into one femoral artery, combined with blood flow measurements, enabled estimation of uptake and release of substrates and metabolites across the leg. Indeed, severe insulin resistance was evident when glucose uptake was assessed across the leg during the EHC (~50% decreased) (Fig. 2g and Extended Data Fig. 2f). In a single very obese pair, leg glucose uptake was virtually without reaction to insulin in either the carrier or control. Indirect calorimetry demonstrated no difference in insulin-stimulated glucose oxidation rates but non-oxidative glucose disposal rates were reduced by ~67% in the carriers (Extended Data Fig. 2g). Taken together, the glucose intolerant phenotype in the carriers is caused by insulin resistance in skeletal muscle and not by insulin resistance in adipose and hepatic tissues. This distinguishes the carriers from most other insulin resistant prediabetic individuals[18,19]. Moreover, the tissue-specific skeletal muscle defect in the carriers illustrates that dysregulated skeletal muscle glucose metabolism per se results in severe whole-body glucose intolerance, insulin resistance and a markedly increased risk of T2D. Although anticipated due to the insulin responsiveness and the large mass of skeletal muscle, this has not previously been documented in humans since most other insulin resistant states involve other organs as well[20]. Notably, our heterogeneous, but paired, participants had a wide BMI span and all carriers, independent of BMI, had impaired glucose tolerance and decreased insulin sensitivity relative to the control participants. In addition, we have previously reported that the carriers are not characterized by higher BMI[1]. This indicates that lifestyle recommendations for the prevention of T2D by weight loss per se may be inadequate in this prediabetic population. We observed severe muscle and whole-body insulin resistance in humans in the absence of baseline hyperinsulinaemia. This indicates that severe peripheral insulin resistance is not counteracted by fasting hyperinsulinaemia (which instead may arise as a result of hepatic insulin resistance).

To illuminate the cellular mechanisms responsible for the muscle insulin resistance, protein content was analysed by global unbiased proteomic analyses of muscle biopsy samples obtained in the rested and non-stimulated state. Due to low statistical power in the proteomic analyses, we subsequently validated some of these findings by targeted immunoblotting. In muscle tissue from the carriers, TBC1D4 protein content was reduced by more than 95% (Fig. 2h,i, Extended Data Fig. 3a and Supplementary Table 2). This was evident in both myosin heavy chain-defined type 1 and type 2 muscle fibres (Extended Data Fig. 3b–d). The homologous TBC1D1 protein was downregulated by ~50% in the carriers (Fig. 2h,i and Supplementary Table 2), which seemed evident in both type 1 and type 2 muscle fibres (Extended Data Fig. 3c,d). In human skeletal muscle, ~50% of TBC1D1 is bound to TBC1D4 (ref. 21) and loss of this binding might contribute to the decreased TBC1D1 protein abundance in muscle of the carriers. However, *TBC1D1* messenger RNA (mRNA) levels were also lower (~30%) in muscle of the carriers and thus, decreased gene transcription may be involved as well (Supplementary Table 3).

Immunoblotting (Fig. 2h and Extended Data Fig. 3a,c,d), proteomics (Fig. 2i and Supplementary Table 2) and confocal microscopy (Extended Data Fig. 3e) analyses revealed that the total GLUT4 protein content was reduced by ~50% in muscle of the carriers. The GLUT4 (*SLC2A4*) mRNA levels were not reduced in muscle of the carriers (Supplementary Table 3), suggesting that GLUT4 protein is subjected to enhanced degradation in the absence of TBC1D4, which is supported by observations in cell culture systems[22]. Also IRAP, a bona fide protein associated with GLUT4 storage vesicles[23–25], was downregulated (Fig. 2h, Extended Data Fig. 3a and Supplementary Table 2), which is in line with observations in a TBC1D1/TBC1D4-deficient mouse model[26]. GLUT1 protein content was normal in muscle of the carriers (Fig. 2h, Extended Data Fig. 3a and Supplementary Table 2), corresponding to findings in TBC1D4-deficient mouse and rat models[26–28]

The protein content of Hexokinase-II (HK-II), glycogen synthase (GS) and pyruvate dehydrogenase (PDH), representing key regulatory enzymes in glucose phosphorylation, storage and oxidation, were unaffected in the carriers. Also, protein content of insulin and exercise signalling proteins upstream of TBC1D4, including the insulin receptor, IRS1, Akt2 and AMP-activated protein kinase (AMPK) were normal in muscle of the carriers (Fig. 2h, Extended Data Fig. 3a–d and Supplementary Table 2).

The ability of insulin to regulate myocellular signalling was evaluated by comparing muscle biopsies obtained before and at the end of the EHC (Fig. 3a). No defect was observed in the phospho-regulation of various proteins related to metabolism including Akt Thr308, p70S6K Thr389 and GS site 3a + 3b or in the activation of GS (Fig. 3b–h and Extended Data Fig. 4a–h). In human muscle, TBC1D4 is phosphorylated on multiple sites during insulin stimulation[12,29,30], and accordingly this regulation was normal in the controls and absent in the carriers. Collectively, our data suggest that skeletal muscle insulin signalling upstream of TBC1D4 is regulated normally in the carriers. Therefore, the compromised insulin-stimulated glucose uptake in muscle of the carriers strongly suggests that the causative defect is distal to or associated with the long isoform of *TBC1D4*. Within the significant top 15 downregulated gene ontology pathways in the proteome, several proteins are related to vesicle trafficking and integrity ('intracellular vesicle', 'CORVET complex', 'COPII vesicle coat' and 'trans-Golgi network transport vesicles') in accordance with the proposed function of TBC1D4 (Extended Data Fig. 4i and Supplementary Table 2).

Whole-body substrate oxidation during fasting, during the glucose challenge and during insulin stimulation (EHC) was similar in both groups (Extended Data Fig. 5a,b). Also, mitochondrial proteins, respiration and proteins related to lipid transport and handling were similar between groups (Fig. 2h, Extended Data Figs. 3a and 5c and Supplementary Table 2). Collectively, this suggests sustained cellular and whole-body metabolic regulation in the carriers.

A single bout of exercise improves muscle glycogen storage[31] and sensitizes muscle glucose uptake to insulin[32]. Current research in animal models suggests that AMPK and TBC1D4 are necessary for this effect[33–35] and it is proposed that TBC1D4 acts as a point of convergence for insulin- (Akt2) and exercise-induced (AMPK) signalling that potentiates insulin-stimulated glucose uptake[33,35–37]. In the carriers, we thus predicted that this insulin-sensitizing effect of exercise would be compromised. To explore this, participants performed one-legged knee-extensor exercise for 1 hour (leaving the contralateral leg as a rested control) and subsequently underwent a 2-hour EHC that was initiated 3 hours into recovery. Insulin-stimulated skeletal muscle glucose uptake was enhanced (~45%) in the previously exercised leg compared to the rested leg in the control participants, demonstrating the insulin-sensitizing effect of exercise (Fig. 3i). In the carriers, this effect was compromised (~50%) but not completely abolished, that is the glucose uptake across the previously exercised leg induced by insulin was increased to the level observed in the rested leg of the controls (Fig. 3i,j and Extended Data Fig. 5d–f). Previous larger human cohorts and animal studies have reported that phospho-regulation of TBC1D4 is enhanced in recovery from exercise[29,33,34,38], and particularly phospho-regulation of Ser704 seems critical for the insulin-sensitizing effect of exercise[39]. This was also evident in four of the five control participants in the present study (Fig. 3g) and suggests that phosphorylation of TBC1D4 is important for the insulin-sensitizing effect of exercise in human skeletal muscle. It is essential to highlight that the necessary role of TBC1D4 for muscle insulin sensitization after exercise

https://doi.org/10.1038/s42255-024-01153-1

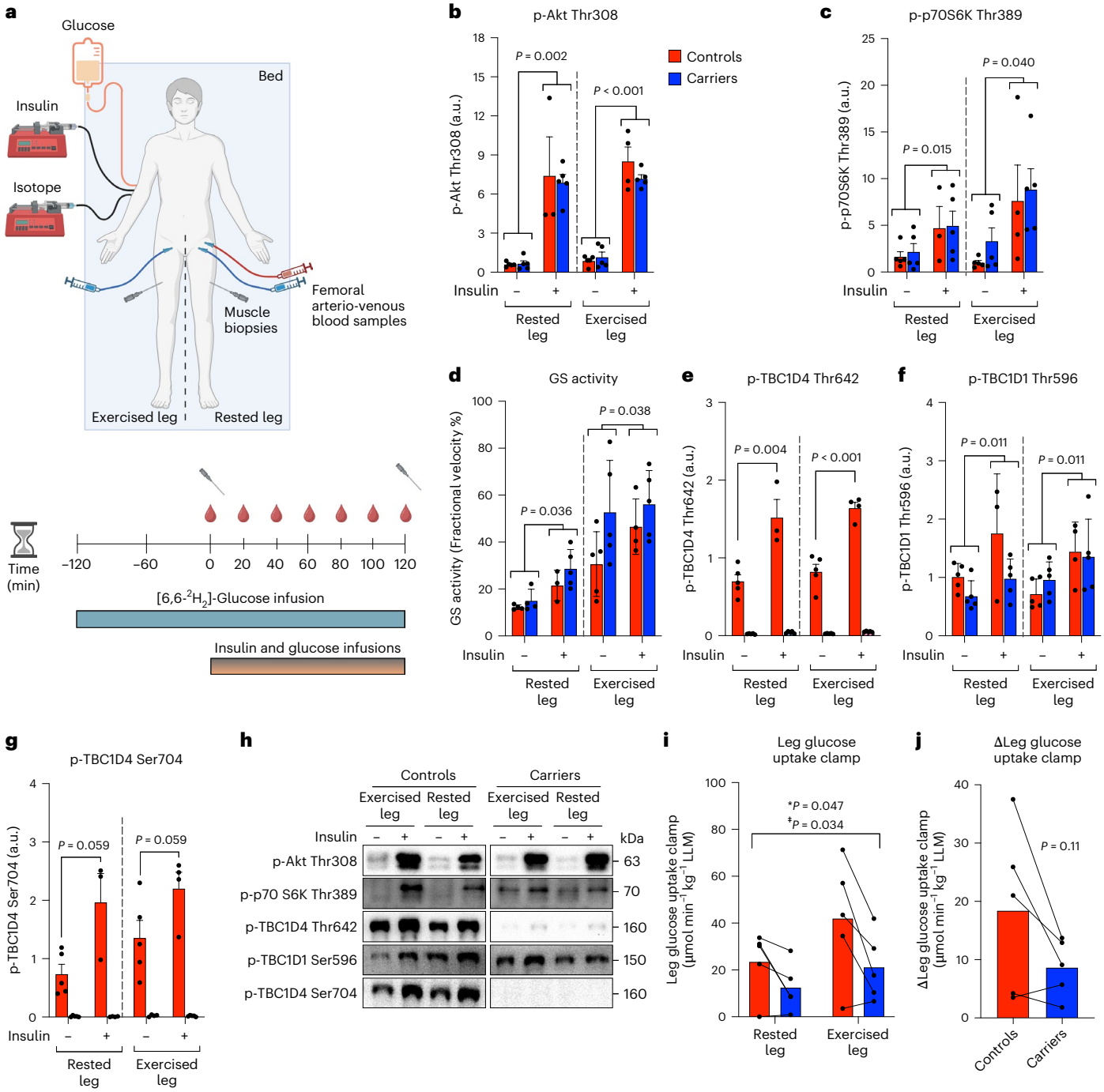

Fig. 3 | Improvement of skeletal muscle insulin resistance by a single bout of exercise in homozygous *TBC1D4* p.Arg684Ter variant carriers. a, Graphical representation of the EHC 3 h into recovery from one-legged knee-extensor exercise. **b**–**g**, Phosphorylation of Akt Thr308 (**b**), p70S6K Thr389 (**c**), TBC1D4 Thr642 (**e**), TBC1D1 Thr596 (**f**) and TBC1D4 Ser704 (**g**) as well as GS activity (**d**) in rested and previously exercised muscle before and at the end of the insulin clamp. **h**, Representative immunoblots. **i**, Average glucose uptake in the rested and exercised leg during the last 40 min of the insulin clamp. **j**, Delta leg glucose uptake (glucose uptake in exercised leg minus glucose uptake in a rested leg). *Difference (main effect) between TBC1D4 carriers and controls. ‡Difference (main effect) between rested and exercised leg. $n = 5$ (rested and exercised leg − insulin), $n = 3$ (rested leg + insulin) and $n = 4$ (exercised leg + insulin) in controls and $n = 5$ in TBC1D4 carriers except for GS activity with $n = 4$ (rested leg − insulin) in controls and TBC1D4 carriers (**b**–**g**). The difference in n is due to missing biopsies as well as depleted sample material. $n = 5$ in controls and in TBC1D4 carriers (**i**,**j**). Data are means ± s.e.m. Data were analysed using a two-tailed paired Student's t-test (**j**) as well as a two-way repeated ANOVA test (two-factor repeated) and two-tailed Student–Newman–Keuls post hoc analyses for multiple comparisons (**b**–**g**, **i**). Graphics in **a** created using BioRender.com. a.u., arbitrary units.

has been demonstrated in muscle with normal GLUT4 protein expression, suggesting that it is the GLUT4 redistribution and translocation process and not GLUT4 protein content per se that is essential for the insulin-sensitizing effect of exercise[34,35]. Moreover, phospho-regulation of signalling upstream of TBC1D4 (that is Akt and AMPK) as well as regulation of GS activity were unaffected in the carriers (Fig. 3b,d and Extended Data Fig. 4a–c,g,h). The fact that the insulin-sensitizing effect of exercise is not completely abolished in the carriers points to

https://doi.org/10.1038/s42255-024-01153-1

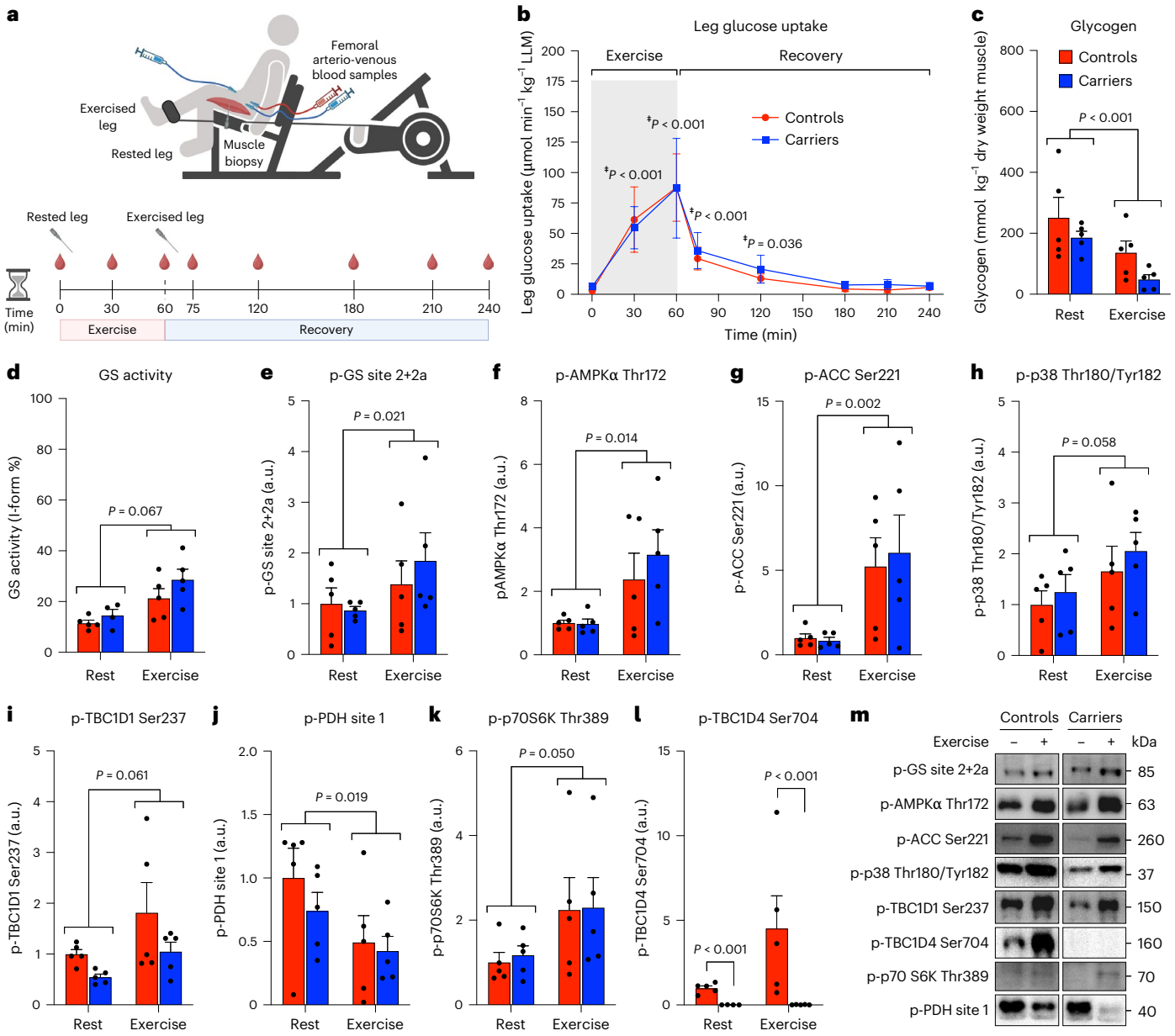

Fig. 4 | Intact skeletal muscle glucose uptake and cellular signalling during exercise in homozygous *TBC1D4* p.Arg684Ter variant carriers. **a**, Graphical representation of the one-legged knee-extensor exercise model. **b**, Leg glucose uptake during 1 h of knee-extensor exercise and 3 h recovery. Leg glucose uptake in a rested leg before exercise: 6.7 ± 3.5 (controls) and 6.4 ± 1.8 (carriers) μmol min^{-1} kg^{-1} LLM. Average leg glucose uptake in a rested leg in exercise recovery: 4.3 ± 1.4 (controls) and 5.5 ± 1.4 (carriers) μmol min^{-1} kg^{-1} LLM. **c**,**d**, Skeletal muscle glycogen content (**c**) and GS activity (**d**) in a rested leg (rest) and exercised leg (exercise). **e**–**l**, Skeletal muscle protein phosphorylation of GS site 2 + 2a (Ser7 + Ser10) (**e**), AMPKα Thr172 (**f**), ACC Ser221 (**g**), P38 Thr180/Tyr182 (**h**), TBC1D1 Ser237 (**i**), PDH site 1 (Ser293) (**j**), p70S6K Thr389 (**k**) and TBC1D4 Ser704 (**l**). **m**, Representative immunoblots. ‡Different from basal (time 0) and rest in both groups (main effects). $n = 5$ in controls and in TBC1D4 carriers. Data are means ± s.e.m. Data were analysed using a two-way repeated ANOVA test (two-factor repeated) and two-tailed Student–Newman–Keuls post hoc analyses for multiple comparisons. Graphics in **a** created using BioRender.com. a.u., arbitrary units.

signalling mechanisms other than TBC1D4 contributing to this phenomenon in humans. Recently, we proposed that mTORC1 is a potential regulator of the glucometabolic action of insulin in skeletal muscle[40]. In the present study, we observed potentiation of the insulin-induced phosphorylation of the mTORC1 target p70S6K Thr389 after exercise (Fig. 3c), aligning with our earlier observations[40]. This regulation was not different between carriers and controls. Thus, in humans mTORC1 may contribute to the insulin-sensitizing effect of exercise.

The TBC1D4 paralogue TBC1D1 as well as GLUT4 are important for regulating muscle glucose uptake both during and in recovery from contraction[37,41–44]. In a transgenic animal model lacking both TBC1D4 and TBC1D1, muscle GLUT4 protein levels were decreased by ~50% leading to impaired contraction-induced glucose uptake[26,45]. We show normal regulation of muscle glucose uptake in the carriers both during and in recovery from exercise (Fig. 4a,b). In line with this finding, leg blood flow, leg arterial-venous glucose difference, blood glucose and plasma levels of lactate, FA, insulin and catecholamines were similar in the carriers and controls during exercise (Extended Data Fig. 6a–h). We observed comparable muscle glycogen levels at rest and similar glycogen use between groups (Fig. 4c). Additionally, phospho-regulation of various exercise-responsive enzymes and signalling components including GS, AMPK, ACC, TBC1D1, p38 MAPK, p70S6K and PDH were

similar between groups (Fig. 4d–k and Extended Data Fig. 6i,j). As expected, phospho-regulation of TBC1D4 was observed only in the control participants (Fig. 4l,m). Furthermore, muscle transcriptomic analyses revealed similar induction of key exercise-responsive genes[46] in the carriers and controls three hours into recovery from exercise (Extended Data Fig. 6k and Supplementary Table 3).

The lack of TBC1D4 in human skeletal muscle, concomitant with a ~50% reduction in both GLUT4 and TBC1D1 protein, did not compromise glucose uptake and metabolic regulation during and in recovery from prolonged submaximal one-legged knee extension exercise. While we did not measure GLUT4 abundance at the cell surface membrane, which is crucial for the muscle glucose transport capacity during exercise[47], it might be speculated that the remaining 50% of GLUT4 is sufficient to drive glucose uptake during exercise as data have shown that only ~25% of the total GLUT4 pool is recruited to the cell surface during muscle contractions[48]. However, manipulation of mouse skeletal muscle GLUT4 and HK-II protein content suggests that glucose phosphorylation, rather than GLUT4 recruitment, is rate limiting for glucose uptake during in vivo exercise[49]. Thus, the normal HK-II content in the carries may secure a normal glucose uptake during and in recovery from exercise.

Here, we reveal the metabolic and molecular consequences of the *TBC1D4* p.Arg684Ter variant in homozygous Greenlandic Inuit carriers. The variant affects the long isoform of *TBC1D4* (refs. 1,6), leading to a lack of TBC1D4 protein in muscle only. Carriers display a normal metabolic phenotype both at the whole-body level and in various organs except for pronounced insulin resistance in skeletal muscle. Dysregulation of TBC1D4 has been linked to insulin resistance because insulin-stimulated phosphorylation of TBC1D4 is impaired in skeletal muscle of individuals with obesity and T2D[9–12]. Animal models have confirmed a role of TBC1D4 for insulin-stimulated glucose uptake, particularly in muscle with decreased GLUT4 protein content[22,26,27,35,50–53]. Insulin resistance in skeletal muscle of rats lacking TBC1D4 is rescued by re-introducing normal GLUT4 protein levels[35]. We propose that the insulin resistance characterizing skeletal muscle lacking TBC1D4 is primarily caused by reduced GLUT4 content, contrasting models with non-phosphorylatable TBC1D4 variants where insulin resistance is caused by disturbed GLUT4 trafficking[50,51]. In primary adipocytes lacking TBC1D4, the lower GLUT4 content seems to be caused by intracellular GLUT4 mis-localization leading to increased lysosomal GLUT4 protein degradation[22].

Knowing the specific characteristics of the insulin resistance in the homozygous p.Arg684Ter carriers might be highly important to lifestyle guidance and prescription of medication for the prevention and treatment of T2D in the carriers. Commonly prescribed medications for patients who have prediabetes or T2D, such as metformin, GLP-1 analogues and the thiazolidinediones, do not directly target skeletal muscle and have only moderate and indirect effects on muscle insulin sensitivity[18,19,54]. In contrast, repeated bouts of exercise (that is, exercise training) is a potent stimuli of muscle insulin sensitivity and GLUT4 expression[55], and we recently found a positive association between self-reported physical activity levels and glycaemic control in the carriers[5]. Thus, it may be speculated that exercise training leading to upregulation of GLUT4 protein rescues insulin action in the carriers. In light of these observations, future research should prioritize conducting dedicated studies to explain the specific mechanisms underlying the benefits of physical training on glycaemia in the carriers.

This study encountered certain challenges during its design and execution, which warrant discussion to enhance the interpretation and validity of our observations. Despite extensive efforts, recruiting additional participants to increase the sample size proved impossible due to the logistical constraints burdening the study. This limitation increases the risk of type 2 errors and warrants caution in interpreting results. The absolute lower insulin levels observed in carriers during the clamp were not significantly different and relates to the insulin level of one control participant. Thus, these data cannot be used to explain decreased insulin action in the carriers, which would contradict the outcomes of the glucose tolerance test and would deviate from findings in preclinical literature. Finally, our findings suggest that muscle-specific insulin resistance is not compensated for by fasting hyperinsulinaemia. Nevertheless, it remains a possibility that this reflects compensatory adaptations in other organs not uncovered by our study.

Methods

Ethical approvals

The study and study protocol were approved by and complies with the ethical regulations of the Commission for Scientific Research in Greenland (project no. 2016-12, document no. 4922964) and the Copenhagen Ethics Committee in Denmark (project no. H-18007316) and conforms to the declaration of Helsinki. The study was registered at Clinical Trial NCT 04170972 before first participant recruitment.

Recruitment in Greenland

Study participants were recruited from the Greenlandic cohort register called the Inuit Health in Transition (IHIT)[56]. Inclusion criteria were: females and males, 25–70 years of age, BMI 20–35 kg m^{-2}, no medical treatment for T2D. No statistical methods were used to predetermine sample size. Sample size was determined by the available number of study participants carrying the TBC1D4 variant. Thus, eight homozygous *TBC1D4* pArg684T variant carriers and eight non-carriers were recruited in Greenland (Extended Data Table 1). The two groups were matched according to age, sex, European genetic admixture, BMI and physical fitness level. Five individually paired participants accepted an invitation for a travel from Nuuk in Greenland to Copenhagen in Denmark to participate in the main experimental day (description below). All study participants were provided oral and written study information after which written informed consent was obtained from all participants before entering the study.

Prescreening and clinical tests in Greenland

Prescreening and clinical tests in Greenland were conducted in our newly established clinical laboratory at Queen Ingrid's Hospital in Nuuk. Fasting blood glucose (ABL90 Flex blood gas analyser, Radiometer), HbA1c (Afinion), body weight and body composition (Inbody 570) were measured during the prescreening of the homozygous carriers and the matched control participants. The clinical tests were performed across 4 days. On day 1, fasting blood samples, whole-body composition and gas exchanges as well as glucose tolerance tests were completed. On day 2, familiarization to a modified Krogh cycle ergometer was performed and peak pulmonary oxygen uptake was estimated. On day 3, a peak workload (PWL) test of the knee extensors was performed and on day 4 tissue biopsies were obtained. The physical tests were separated by at least 2 days.

Glucose tolerance was measured during a prolonged 6-h OGTT. One carrier experienced discomfort and did not complete the glucose tolerance test. After overnight fasting, participants arrived at the laboratory and rested for 30 min. Oxygen uptake and respiratory exchange ratio (RER; reflecting substrate use) were measured during the resting period (Vyntus CPX, Vyaire Medical, installed with SentrySuite software v.3.20.8) followed by insertion of a venflon in a dorsal hand vein (Venflon Pro Safety, Mediq). Following the 30 min of rest, a fasting blood sample was collected (time 0). Immediately after, 75 g glucose diluted in 250 ml water (Pharmacy, Region Hospital, Copenhagen, Denmark) was consumed during a 5-min period. After glucose intake, blood samples were collected at times of 30, 60, 90, 120, 150, 180, 240, 300 and 360 min for measurement of blood glucose (ABL90 Flex blood gas analyser, Radiometer), FA and hormones. Oxygen uptake and RER were measured at 30, 120, 240 and 330 min.

Peak pulmonary oxygen uptake (VO_2 peak) was estimated using a two-level submaximal cycle ergometer test (Monark ergometer cycle,

839E, Vansbro) with measurement of heart rate and oxygen uptake (Vyntus CPX, Vyaire Medical GmbH) during steady state conditions[57].

Familiarization to a modified Krogh cycle ergometer, which allows dynamic contractions of only the knee extensor, and a PWL test of the knee extensors on the Krogh ergometer were performed as previously described[58].

Participants arrived at the laboratory in the fasted state to have a muscle biopsy taken from m. vastus lateralis in one leg as well as an abdominal subcutaneous adipose tissue biopsy. Biopsies were obtained under local anaesthesia (~3 ml Xylocaine 2%, AstraZeneca) using the Bergström needle technique with suction.

Experimental day in Denmark

After the recruitment, prescreening and initial clinical tests in Greenland, the participants were invited to Denmark for engagement in the main experimental day. During their stay in Denmark, all participants were accommodated at the same hotel in Copenhagen. Participants abstained from alcohol and strenuous physical activity and were on a standardized diet (55 E% CHO, 30 E% fat, 15 E% protein) for 3 days preceding the main experimental day. During the stay, lean leg mass (LLM) was measured by dual X-ray absorptiometry (DPX-IQ Lunar, Lunar Corporation) and data analysed with Lunar Prodigy Advance Encore software v.16.

On the experimental day, participants abstained from caffeine (previous 24 h) and arrived at the laboratory 1 h after having ingested a light breakfast (5% of daily energy intake; Greek yoghurt, blueberries and almonds). After 30 min of rest, catheters were placed in both femoral veins and in one femoral artery (Pediatric Jugular Catheterization set, Arrow International). The catheters were used for obtaining multiple blood samples from both femoral veins and artery during exercise, in the recovery period after exercise and during a EHC. This allowed estimation of arterial-venous differences of various substances including glucose. Arterial blood flow in both legs was estimated by Doppler Ultrasound (Philips iU22, ViCare Medical A/S). Uptake and release of substrates to/from the leg were calculated using Fick's principle and related to LLM. Whole-body oxygen uptake and RER as well as leg substrate balance and blood flow were measured after 60 min of rest. A muscle biopsy was obtained from m. vastus lateralis from one leg (rested leg) under local anesthaesia (~3 ml of Xylocaine 2%, AstraZeneca) using the Bergström needle technique immediately before initiation of exercise. The exercise consisted of one-legged knee-extensor exercise for 1 h at 80% PWL leaving the contralateral leg as a rested control. Whole-body oxygen uptake and RER (at 20 and 50 min) as well as leg substrate balance and blood flow (at 30 and 60 min) were measured during the exercise period. Immediately after exercise, a muscle biopsy from the exercised leg was obtained. Then the participants rested in the fasted state for 3 h. In this period, whole-body oxygen uptake and substrate use (at 30 and 60 min) as well as leg substrate balance and blood flow (at 15, 60, 150 and 180 min) were measured. During the resting period, antecubital catheters (Venflon Pro Safety, Mediq) were inserted in both arms. During the last 2 hours of the recovery period, [6,6-$^2H_2$]-glucose (Cambridge Isotope Laboratories) was infused with a constant rate of 0.044 mg kg^{-1} min^{-1}. By the end of the resting period, biopsies were obtained from m. vastus lateralis of both legs. Then a 2 h EHC was initiated to evaluate insulin sensitivity. The clamp was initiated by a bolus injection of insulin (9 mU kg^{-1}, Actrapid, Novo Nordisk) followed by 120 min of constant insulin infusion (1.42 mU min^{-1} kg^{-1}). Glucose was infused during the EHC from a 20% glucose solution enriched with 1.9% [6,6-$^2H_2$]-glucose. The infusion rate was adjusted throughout the clamp to maintain euglycaemia (~5–6 mM). Blood samples were drawn from all three leg catheters immediately before (0 min) and during the EHC (20, 40, 60, 80, 100 and 120 min) and blood flow was measured concurrently. By the end of the clamp, muscle biopsies of m. vastus lateralis were obtained from both legs. In one control participant, a biopsy was not obtained in the rested leg by the end of the clamp while in another control participant, a biopsy was not obtained in the exercised leg by the end of the clamp. Arterial blood samples were obtained by the end of the rest period, by 30 and 120 min of the EHC for estimation of the enrichment of [6,6-$^2H_2$]-glucose used to calculate hepatic glucose production.

The investigators were not blinded to the group allocation (TBC1D4 variant versus control) because all study participants were genotyped before entering the study. Part of the data collection was performed blinded including blood analyses of hormones, enzyme activities, mitochondrial respirometry, GLUT4 imaging, RNA sequencing (RNA-seq) and proteomics while other parts of the data collection were performed non-blinded including immunoblotting analyses. Randomization was not applied because all participants underwent the same experimental procedure.

Western blotting on skeletal muscle homogenates, lysates and single fibres

Homogenate and lysate SDS–PAGE and western blot analyses were performed as previously described[59]. In short, an aliquot of each muscle biopsy sample was prepared and boiled in Laemmli buffer before being subjected to SDS–PAGE on self-cast Tris-HCl polyacrylamide gels. Proteins were transferred to a polyvinyl difluoride membrane (Immobilon Transfer Membranes; Millipore) by semidry blotting. Membranes were blocked in TBST (10 mM Tris-base, 150 mM NaCl and 0.25% Tween 20) containing low fat milk (2–3%) protein or bovine serum albumin (BSA; 3%) and then probed with primary antibodies and appropriate secondary antibodies. The antibodies used are listed in Supplementary Table 4. Protein bands were visualized using enhanced chemiluminescence (Immobilon Forte Western HRP substrate, MerckMillipore or SuperSignal West Femto Maximum Sensitivity Substrate, ThermoFisher Scientific), and a ChemiDoc MP imaging system (BioRad). Band quantification was performed using BioRad Image Lab v.6.0.1. To ensure uniformity, individual samples, standards and protein ladder from different gels were transferred to a single membrane for subsequent quantification and statistical analyses. Some membranes were stripped in a buffer containing 100 mM 2-mercaptoethanol, 2% SDS and 62.5 mM Tris-HCl. After checking for successful removal of the primary antibody, the membranes were reprobed with a new primary antibody. Single fibre preparation, fibre type determination, myosin heavy chain distribution and western blot analysis on pooled single fibres from each participant were performed as previously described[60]. All membranes used for western blotting on lysates, homogenates and single fibres were checked for equal total protein loading and transfer by Coomassie or membrane stain kit (MemCode Reversible Protein Stain Kit, Thermo Scientific, no. 24585).

Blood analyses

Blood glucose and lactate levels were measured by a blood gas analyser (ABL800 FLEX, Radiometer). For [6,6-$^2H_2$]-glucose, plasma enrichment of [6,6-$^2H_2$]-glucose was measured using liquid chromatography mass spectrometry as previously described[61]. The concentration of FA (NEFA C kit, Wako Chemicals), triacylglycerol (GPO-PAP kit, Roche Diagnostics), glycerol (Randox) and total, HDL and LDL cholesterol (Roche Diagnostics) in plasma were measured using colorimetric methods on an autoanalyser (Pentra C400, Horiba Medical). For insulin, plasma concentrations were measured by enzyme-linked immunosorbent assay (ELISA) (no. 80-INSHU-E01.1, ALPCO). For C-peptide, plasma concentrations were measured by ELISA (ALPCO). The plasma concentrations for glucagon (cat. no. 10-1271-01), total GLP-1 (cat. no. 10-1278-01) and total GIP (cat. no. 10-1258-01) were quantified by ELISA in duplicate (Mercodia) and run on a SpectraMax iD3. For adrenalin and noradrenalin, the plasma concentrations were measured using a 2-CAT Plasma ELISA$^{\text{High Sensitive}}$ kit (Labor Diagnostika Nord GmbH & Co). For cortisol and growth hormone, the plasma concentrations were

measured using antibody-based assays (Elecsys Cortisol II and Elecsys hGH) automated on a Cobas 8000 (Roche).

Glycogen content

Muscle glycogen content was measured in muscle homogenates as glycosyl units after acid hydrolysis[62].

GS activity

GS activity was measured in homogenates as previously described[63] and presented as the %I-form (enzyme activity assayed in the presence of 0.02 mM glucose-6-phosphate (G6P) given relative to enzyme activity in the presence of saturating conditions (8 mM G6P)).

GLUT4 imaging

Immediately after the muscle biopsy procedure, a piece of the muscle was immersed in an ice-cooled 0.1 M sodium phosphate buffer solution (pH 7.4) containing 4% paraformaldehyde and 0.05% glutaraldehyde for fixation. On ice, the muscle samples were finely divided into smaller bundles of <30 fibres and incubated shaking for 4 h. Fixed samples were stored in phosphate buffer containing 1% paraformaldehyde and 50% glycerol at 4 °C until use. For staining, four to six individual fibres were teased out from the fixed fibre bundles with fine forceps and blocked for 2 h in PBS containing 5% goat serum, 1% BSA and 0.04% saponin and then incubated overnight with primary antibody raised against GLUT4 (rabbit polyclonal; no. PA5-23052; lot WJ3403509, Thermo Scientific). Next day, fibres were washed three times for 10 min in PBS containing 0.04% saponin and incubated with secondary antibody conjugated to Alexa 568 for 2 h followed by another three times for 10 min to wash. Subsequently, the fibres were mounted in Vectashield (Vector Laboratories, Inc.). Images were collected using a LSM710 (Carl Zeiss) through a ×63/1.40 oil DIC III Plan-Apochromat objective at 20 °C and Zeiss Zen Black 2012 software. Total GLUT4 content was quantified using ImageJ[64]. Image collection and quantification were performed blinded.

Mitochondrial respirometry in permeabilized muscle fibres

Skeletal muscle mitochondrial respiration was measured in a subset of the study participants ($n = 5$ per group). A portion of the muscle biopsies was placed in ice-cold BIOPS buffer (50 mM MES, 7.23 mM Ca-EGTA, 2.77 mM CaK_2EGTA, 20 mM imidazole, 20 mM taurine, 5.7 mM ATP, 14.3 mM phosphocreatine, 6.56 mM $MgCl_2$, pH 7.1). Muscle fibres were then divided into bundles of 1–3 mg and teased out using fine forceps to minimize oxygen diffusion limitations during respirometry. Fibres were permeabilized in 30 µg ml^{-1} saponin for 30 min at 4 °C followed by washing in ice-cold mitochondrial respiration buffer (0.5 mM EGTA, 3 mM $MgCl_2$, 60 mM lactobionate, 20 mM taurine, 10 mM KH_2PO_4, 20 mM HEPES and 110 mM D-sucrose, with 1 g l^{-1} BSA) for 30 min before analysis. We analysed oxygen consumption in duplicates using the Oxygraph-2k system (Oroboros Instruments, installed with Oroboros Datlab v.7.0) at 37 °C with O_2 concentration kept at 200–450 µM.

The respirometry protocol consisted of sequential addition of 5 mM pyruvate, 10 mM glutamate and 2 mM malate followed by addition of 4 mM ADP to assess Complex I-linked state 3 respiration. This was followed by addition of cytochrome C as a quality control for outer mitochondrial membrane integrity. Maximal Complex I + II-linked state 3 respiratory capacity was measured by addition of 10 mM succinate, which was followed by addition of FCCP and subsequently 0.5 µM rotenone to assess maximal uncoupled respiration (that is, maximal electron transfer capacity) supported by either Complex I + II or Complex II alone.

Given that the Inuit population may have been under selective pressure towards enhanced fat oxidation capacity, the *TBC1D4* p.Arg684Ter variant may have mitochondrial effects that are unique to fat oxidation. Therefore, the respirometry protocol was repeated with the additional presence of FAs (0.04 mM palmitoylcarnitine and 0.5 mM octanoylcarnitine).

RNA-seq

RNA was purified from roughly 12 mg wet weight skeletal muscle and roughly 50 mg wet weight subcutaneous abdominal adipose tissue. Using a Retsch TissueLyserII (Qiagen) frozen muscle and adipose tissue was homogenized in 700 and 1,200 µl of TRIzol (ThermoFisher), respectively. After purification, the RNA was dissolved in 0.1 mM EDTA in DEPC with 1 µl mg^{-1} for muscle tissue and 10 µl in total for all adipose samples. One microlitre of each sample was used for determination of RNA concentration and integrity in an Agilent 2100 bio-analyser (Agilent). The RNA-seq data quality was assessed using FastQC (https://www.bioinformatics.babraham.ac.uk/projects/fastqc/). The raw paired-end sequencing data match the expectation for human RNA-seq data, with the exception of sample 2F, which had elevated GC content with a mode at 61% GC. Sequencing data for each sample were aligned to the human reference genome (GRCh38.p13) indexed with Gencode (v.34) using STAR (v.2.7.9a, default parameters)[65]. Sample 2F was excluded from downstream analyses as the expected GC content with a mode ~42–46% could not be recovered after mapping. To ensure the RNA integrity, we quantified the RNA degradation (TIN score) for each sample[66]. Due to a low TIN score <60, sample 33F was excluded from downstream analyses. For the remaining 54 samples, gene count and transcripts per million quantification were obtained using RNA-SeQC2 (v.2.3.4, default parameters) considering only uniquely mapped reads[67]. In total, 58,264 transcripts were quantified. All RNA-seq data after preprocessing from both adipose tissue and muscle biopsies were analysed with DESeq2 (ref. 68) in R v.4.0.2 (https://www.R-project.org/) using standard recommended settings as given in the DESeq2 documentation wherever possible.

Proteomics

Sample preparation. Frozen muscle biopsies (~20 mg wet weight) were ground in liquid nitrogen with a mortar and pestle. The ground biopsies were lysed in 200 µl of 6 M GdmCl/100 mM Tris pH 8.5, sonicated (5 min, 90% amplitude, 2 s/5 s pulses, 4 °C) in a Q800R2 (QSonica) and immediately boiled (95 °C, 5 min). Lysates were sonicated (1 min, 90% amplitude, 5 s/5 s pulses, 4 °C) and centrifuged at 20,000*g* for 5 min. Supernatants were reduced and alkylated with 10 mM TCEP/40 mM CAA (5 min at 45 °C followed by 40 min at room temperature). Protein was precipitated with chloroform:methanol (4:8 volumes of the supernatant), and pellets were resolubilized with 1% SDC/100 mM Tris pH 8.5. Protein concentration was determined with a BCA assay, and 80 µg of each sample was digested with 1:50 trypsin and Lys-C (37 °C, 2,000 rpm, 18 h). Peptides were diluted 1:1 in water and then cleaned up on 6× SDB–RPS stage tips with two washes in 1% trifluoroacetic acid (TFA) 99% ethyl acetate, followed by a wash in 1% TFA 99% isopropanol then 0.2% TFA 5% acetonitrile (ACN). Peptides were eluted in 0.125% NH_4OH 60% ACN, then concentrated under vacuum (45 °C, 90 min).

High-pH reverse phase fractionation. Peptides from each muscle biopsy were fractionated as described[69] with minor modifications. Peptides were resuspended in 100 µl of MS loading buffer (2% ACN 0.3% TFA) and fractionated using a Dionex UltiMate 3000 high-performance liquid chromatography (HPLC) using an XBridge Peptide BEH C18 column (130 Å, 3.5 µm, 2.1 × 250 mm). The column was maintained at 50 °C during fractionation. Buffer A comprised 10 mM ammonium formate/2% ACN and buffer B 10 mM ammonium formate/80% ACN. Both buffers were adjusted to pH 9.0 with NH_4OH. Peptides were separated with a gradient of 10–40% buffer B over 4.4 min, followed by 40–100% buffer B over 1 min. Seventy-two fractions were collected with concatenation during collection after 24 samples, such that fractions 1, 25 and 49 were pooled (as were fractions 2, 26 and 50 and so on). After fraction collection samples were dried down directly in the deep-well plate using a vacuum concentrator.

DIA LC–MS/MS analysis. Fractionated peptides were resuspended in 5 µl MS loading buffer (2% ACN 0.3% TFA) and loaded onto a 150 µm ID × 15 cm column packed in-house with 1.9 µm of C18 material (Repro-Sil Pur AQ C18, Dr. Maisch, GmbH) using an EvoSep HPLC. Column temperature was maintained at 60 °C using a column oven (Sonation). An EvoSep One (EvoSep) HPLC was interfaced with an Orbitrap Exploris 480 mass spectrometer (ThermoFisher Scientific) and peptides were separated using a binary buffer system comprising 0.1% formic acid (buffer A) and ACN plus 0.1% formic acid (buffer B) using the standard 30 samples per day method, resulting in MS acquisition times of 44 min plus overheads of ~2 min per sample. Peptides were analysed with one full scan (350–1,400 *m/z*, $R = 120{,}000$) at a target of 3×10^6 ions, followed by 48 data-independent acquisition (DIA) MS/MS scans (350–1,022 *m/z*) with higher energy collisional dissociation (target 3×10^6 ions, max injection time 22 ms, isolation window 14 *m/z*, 1 *m/z* window overlap, normalized collision energy (NCE) 25%), with fragments detected in the Orbitrap ($R = 15{,}000$).

RAW data processing. RAW data was analysed using MaxQuant (v.2.1.3.0), with searches performed against the Human UniProt Reference database (May 2021) using Discovery DIA libraries as described[70]. Default settings were used, with the addition of the 'match between runs' setting for adjacent and/or matching fractions (matching time window 0.7) and intensity-based absolute quantification.

Statistics and bioinformatics

General information. No data points were removed from the analysis. However, there are missing data points due to insufficient tissue availability related to smaller tissue biopsies. Data distribution was assumed to be normal but was not formally tested given the small sample size. Due to the low sample size in our data, we found it inappropriate to disaggregate our data for sex. Investigators were blinded during data analysis but not blinded during the statistical analyses.

RNA-seq. To test for differential expression, DESeq2 relies on a linear regression model, which was performed several times with different settings but always with the pairing scheme as a cofactor. This gave rise to the three distinct datasets presented in Supplementary Tables 1 and 3. In that order, the data were obtained as follows: differential expression data obtained from RNA-seq of the adipose tissue samples with or without insulin stimulation were derived using DESeq2 linear regression with *P* values obtained from the interaction between TBC1D4 control or carrier and clamp before or after using the participant-pairing scheme as a cofactor (Supplementary Table 1). The RNA-seq of the skeletal muscle tissues of TBC1D4 controls and carriers gave rise to two datasets obtained by twice applying the linear regression models of DESeq2. First, *P* values were obtained from data at rest before exercise by comparing TBC1D4 reference versus carriers using the pairing scheme as a cofactor (Supplementary Table 3). Second, *P* values were obtained from the interaction between TBC1D4 reference or carriers and exercise before or after using the participant-pairing scheme as a cofactor (Supplementary Table 3). A gene set enrichment analysis (GSEA)[71,72] was performed using the classical preranked approach on the rankings provided by the *P* values from the three models described above. The analysis was performed using the GSEA tool (v.4.3.2) (https://www.gsea-msigdb.org/gsea) with default settings on the Kyoto Encyclopedia of Genes and Genomes database gene set (https://data.broadinstitute.org/gsea-msigdb/msigdb/release/2023.1.Hs/c2.cp.kegg.v2023.1.Hs.symbols.gmt).

Proteomics. Protein intensities were log-transformed and median-normalized. To test for differential protein abundances between participants with and without the *TBC1D4* p.Arg684Ter variant, paired *t*-tests were performed with participant pairing according to the matched carriers and controls. Empirical Bayes moderated *t*-statistics were calculated, implemented in the LIMMA R package[73]. *P* values were adjusted for multiple hypothesis testing with the Benjamini–Hochberg method[74]. To calculate enrichment of regulated proteins in Gene Ontology Cellular Components, a modified weighted GSEA method was used, as implemented in the ksea R package[75].

Other statistical analyses. Statistical analyses of data not related to proteomics and RNA-seq were performed using SigmaPlot software (v.4.0, SYSTAT). Data are presented as means ± s.e.m. unless stated otherwise and all bar graphs are presented with individual values. Paired and unpaired Student's *t*-tests were used for two-group comparisons. Two-way repeated analysis of variance (ANOVA) tests (one or two-factor repeated) were used to compare two independent variables followed by Student–Newman–Keuls post hoc analyses for multiple comparisons. Statistical significance was defined as $P < 0.05$. Before commencing the study, meticulous efforts were made to individually match participants in pairs, taking into account various parameters known to have an influence on the study's outcome. As a consequence of this pre-established pairing, we performed paired statistical analyses on the dataset, thereby ensuring that comparisons were made within the context of these individually matched pairs. This statistical procedure has been validated by independent statisticians at the Department of Mathematical Sciences, University of Copenhagen.

Calculations. The adipose tissue insulin-resistance index was calculated as (fasting serum insulin (µU ml^{-1})) × (log(fasting serum FA (µmol l^{-1})[76]. $ISI_{0,120}$ (insulin sensitivity index) was calculated as described previously[77]. The HOMA-IR index was calculated as (fasting serum insulin (µU ml^{-1})) × (fasting plasma glucose (mM l^{-1}))/22.5. Genetic EU-admixture was assessed as previously described[1] and leg glucose uptake was calculated as (arterial blood flow (l min^{-1})) × (arterial-venous glucose difference (mM l^{-1})) and related to the leg lean mass (kg).

Reporting summary

Further information on research design is available in the Nature Portfolio Reporting Summary linked to this article.

Data availability

RAW data and processed output tables have been deposited in the PRIDE proteomeXchange repository and can be accessed at https://www.ebi.ac.uk/pride/ with the accession PXD045301. Raw RNA-seq reads produced in this work have been deposited to the European Genome-phenome Archive database, accession number EGAD50000000059. Source data are provided with this paper. All other data that support the findings of this study are available from the corresponding author upon reasonable request to ensure confidentiality and privacy for the study participants.

References

1. Moltke, I. et al. A common Greenlandic TBC1D4 variant confers muscle insulin resistance and type 2 diabetes. *Nature* **512**, 190–193 (2014).
2. Jorgensen, M. E. et al. Diabetes and impaired glucose tolerance among the inuit population of Greenland. *Diabetes Care* **25**, 1766–1771 (2002).
3. Dahl Petersen, I. K., Bjerregaard, P. & Jørgensen, M. E. Physical activity patterns in Greenland: a country in transition. *Scand. J. Public Health* **39**, 678–686 (2011).
4. Dahl-Petersen, I. K., Bjerregaard, P., Brage, S. & Jørgensen, M. E. Physical activity energy expenditure is associated with 2-h insulin independently of obesity among Inuit in Greenland. *Diabetes Res. Clin. Pract.* **102**, 242–249 (2013).
5. Schnurr, T. M. et al. Physical activity attenuates postprandial hyperglycaemia in homozygous TBC1D4 loss-of-function mutation carriers. *Diabetologia* **64**, 1795–1804 (2021).

6. Baus, D. et al. Identification of a novel AS160 splice variant that regulates GLUT4 translocation and glucose-uptake in rat muscle cells. *Cell. Signal.* **20**, 2237–2246 (2008).
7. Espelage, L., Al-Hasani, H. & Chadt, A. RabGAPs in skeletal muscle function and exercise. *J. Mol. Endocrinol.* **64**, R1–R19 (2020).
8. Mafakheri, S., Chadt, A. & Al-Hasani, H. Regulation of RabGAPs involved in insulin action. *Biochem. Soc. Trans.* **46**, 683–690 (2018).
9. Karlsson, H. K. R. et al. Insulin-stimulated phosphorylation of the Akt substrate AS160 is impaired in skeletal muscle of type 2 diabetic subjects. *Diabetes* **54**, 1692–1697 (2005).
10. Højlund, K. et al. Impaired insulin-stimulated phosphorylation of akt and AS160 in skeletal muscle of women with polycystic ovary syndrome is reversed by pioglitazone treatment. *Diabetes* **57**, 357–366 (2008).
11. Vind, B. F. et al. Impaired insulin-induced site-specific phosphorylation of TBC1 domain family, member 4 (TBC1D4) in skeletal muscle of type 2 diabetes patients is restored by endurance exercise-training. *Diabetologia* **54**, 157–167 (2011).
12. Middelbeek, R. J. W. et al. Insulin stimulation regulates AS160 and TBC1D1 phosphorylation sites in human skeletal muscle. *Nutr. Diabetes* **3**, e74 (2013).
13. Heller, S. R. et al. Risk of hypoglycaemia in types 1 and 2 diabetes: effects of treatment modalities and their duration. *Diabetologia* **50**, 1140–1147 (2007).
14. Lupoli, R. et al. Role of the entero-insular axis in the pathogenesis of idiopathic reactive hypoglycemia: a pilot study. *J. Clin. Endocrinol. Metab.* **100**, 4441–4446 (2015).
15. Ghosh, C., Mukhopadhyay, P., Ghosh, S. & Pradhan, M. Insulin sensitivity index (ISI0, 120) potentially linked to carbon isotopes of breath CO2 for pre-diabetes and type 2 diabetes. *Sci. Rep.* **5**, 11959 (2015).
16. Heller, S. R. et al. A higher non-severe hypoglycaemia rate is associated with an increased risk of subsequent severe hypoglycaemia and major adverse cardiovascular events in individuals with type 2 diabetes in the LEADER study. *Diabetologia* **65**, 55–64 (2022).
17. Overvad, M. et al. The effect of diabetes and the common diabetogenic TBC1D4 p.Arg684Ter variant on cardiovascular risk in Inuit in Greenland. *Sci. Rep.* **10**, 22081 (2020).
18. Kanat, M., DeFronzo, R. A. & Abdul-Ghani, M. A. Treatment of prediabetes. *World J. Diabetes* **6**, 1207 (2015).
19. DeFronzo, R. A. et al. Type 2 diabetes mellitus. *Nat. Rev. Dis. Prim.* **1**, 15019 (2015).
20. James, D. E., Stöckli, J. & Birnbaum, M. J. The aetiology and molecular landscape of insulin resistance. *Nat. Rev. Mol. Cell Biol.* **22**, 751–771 (2021).
21. Larsen, J. K. et al. Illumination of the endogenous insulin-regulated TBC1D4 interactome in human skeletal muscle. *Diabetes* **71**, 906–920 (2022).
22. Xie, B. et al. The inactivation of RabGAP function of AS160 promotes lysosomal degradation of glut4 and causes postprandial hyperglycemia and hyperinsulinemia. *Diabetes* **65**, 3327–3340 (2016).
23. Larance, M. et al. Characterization of the role of the Rab GTPase-activating protein AS160 in insulin-regulated GLUT4 trafficking. *J. Biol. Chem.* **280**, 37803–37813 (2005).
24. Peck, G. R. et al. Interaction of the Akt substrate, AS160, with the glucose transporter 4 vesicle marker protein, insulin-regulated aminopeptidase. *Mol. Endocrinol.* **20**, 2576–2583 (2006).
25. Eickelschulte, S. et al. AKT/AMPK-mediated phosphorylation of TBC1D4 disrupts the interaction with insulin-regulated aminopeptidase. *J. Biol. Chem.* **296**, 100637 (2021).
26. Chadt, A. et al. Deletion of both rab-GTPase-activating proteins TBC1D1 and TBC1D4 in mice eliminates insulin- and AICAR-stimulated glucose transport. *Diabetes* **64**, 746–759 (2015).
27. Lansey, M. N., Walker, N. N., Hargett, S. R., Stevens, J. R. & Keller, S. R. Deletion of Rab GAP AS160 modifies glucose uptake and GLUT4 translocation in primary skeletal muscles and adipocytes and impairs glucose homeostasis. *Am. J. Physiol. Endocrinol. Metab.* **303**, E1273–E1286 (2012).
28. Arias, E. B., Zheng, X., Agrawal, S. & Cartee, G. D. Whole body glucoregulation and tissue-specific glucose uptake in a novel Akt substrate of 160 kDa knockout rat model. *PLoS ONE* **14**, e0216236 (2019).
29. Treebak, J. T. et al. Potential role of TBC1D4 in enhanced post-exercise insulin action in human skeletal muscle. *Diabetologia* **52**, 891–900 (2009).
30. Vendelbo, M. H. et al. Insulin resistance after a 72-h fast is associated with impaired AS160 phosphorylation and accumulation of lipid and glycogen in human skeletal muscle. *Am. J. Physiol. Endocrinol. Metab.* **302**, E190–E200 (2012).
31. Bergström, J. & Hultman, E. Muscle glycogen synthesis after exercise: an enhancing factor localized to the muscle cells in man.*Nature* **210**, 309–310 (1966).
32. Richter, E. A., Mikines, K. J., Galbo, H. & Kiens, B. Effect of exercise on insulin action in human skeletal muscle. *J. Appl. Physiol.* **66**, 876–885 (1989).
33. Kjøbsted, R. et al. Enhanced muscle insulin sensitivity after contraction/exercise is mediated by AMPK. *Diabetes* **66**, 598–612 (2017).
34. Kjøbsted, R. et al. TBC1D4 is necessary for enhancing muscle insulin sensitivity in response to AICAR and contraction. *Diabetes* **68**, 1756–1766 (2019).
35. Zheng, A. et al. Exercise-induced improvement in insulin-stimulated glucose uptake by rat skeletal muscle is absent in male AS160-Knockout rats, partially restored by muscle expression of phosphomutated AS160, and fully restored by muscle expression of wild-type AS160. *Diabetes* **71**, 219–232 (2022).
36. Cartee, G. D. & Wojtaszewski, J. F. P. Role of Akt substrate of 160 kDa in insulin-stimulated and contraction-stimulated glucose transport. *Appl. Physiol. Nutr. Metab.* **32**, 557–566 (2007).
37. Kjøbsted, R. et al. AMPK and TBC1D1 regulate muscle glucose uptake after, but not during, exercise and contraction. *Diabetes* **68**, 1427–1440 (2019).
38. Steenberg, D. E. et al. A single bout of one-legged exercise to local exhaustion decreases insulin action in nonexercised muscle leading to decreased whole-body insulin action. *Diabetes* **69**, 578–590 (2020).
39. Kjøbsted, R. et al. TBC1D4-S711 controls skeletal muscle insulin sensitization after exercise and contraction. *Diabetes* **72**, 857–871 (2023).
40. Needham, E. J. et al. Personalized phosphoproteomics identifies functional signaling. *Nat. Biotechnol.* **40**, 576–584 (2022).
41. An, D. et al. TBC1D1 regulates insulin- and contraction-induced glucose transport in mouse skeletal muscle. *Diabetes* **59**, 1358–1365 (2010).
42. Vichaiwong, K. et al. Contraction regulates site-specific phosphorylation of TBC1D1 in skeletal muscle. *Biochem. J.* **431**, 311–320 (2010).
43. Stöckli, J. et al. The RabGAP TBC1D1 plays a central role in exercise-regulated glucose metabolism in skeletal muscle. *Diabetes* **64**, 1914–1922 (2015).
44. Zisman, A. et al. Targeted disruption of the glucose transporter 4 selectively in muscle causes insulin resistance and glucose intolerance. *Nat. Med.* **6**, 924–928 (2000).
45. Wendt, C. D. et al. Contraction-mediated glucose transport in skeletal muscle is regulated by a framework of AMPK, TBC1D1/4, and Rac1. *Diabetes* **70**, 2796–2809 (2021).

46. Pillon, N. J. et al. Transcriptomic profiling of skeletal muscle adaptations to exercise and inactivity. *Nat. Commun.* **11**, 470 (2020).
47. Klip, A., McGraw, T. E. & James, D. E. Thirty sweet years of GLUT4. *J. Biol. Chem.* **294**, 11369–11381 (2019).
48. Ploug, T., Van Deurs, B., Ai, H., Cushman, S. W. & Ralston, E. Analysis of GLUT4 distribution in whole skeletal muscle fibers: Identification of distinct storage compartments that are recruited by insulin and muscle contractions. *J. Cell Biol.* **142**, 1429–1446 (1998).
49. Wasserman, D. H., Kang, L., Ayala, J. E., Fueger, P. T. & Lee-Young, R. S. The physiological regulation of glucose flux into muscle in vivo. *J. Exp. Biol.* **214**, 254–262 (2011).
50. Kramer, H. F. et al. AS160 regulates insulin- and contraction-stimulated glucose uptake in mouse skeletal muscle. *J. Biol. Chem.* **281**, 31478–31485 (2006).
51. Chen, S., Wasserman, D. H., MacKintosh, C. & Sakamoto, K. Mice with AS160/TBC1D4-Thr649Ala knockin mutation are glucose intolerant with reduced insulin sensitivity and altered GLUT4 trafficking. *Cell Metab.* **13**, 68–79 (2011).
52. Yang, X. et al. Tissue-specific splicing and dietary interaction of a mutant As160 allele determine muscle metabolic fitness in rodents. *Diabetes* **70**, 1826–1842 (2021).
53. Wang, H. Y. et al. AS160 deficiency causes whole-body insulin resistance via composite effects in multiple tissues. *Biochem. J* **449**, 479–489 (2013).
54. Mastrototaro, L. & Roden, M. Insulin resistance and insulin sensitizing agents. *Metabolism.* **125**, 154892 (2021).
55. Richter, E. A. & Hargreaves, M. Exercise, GLUT4, and skeletal muscle glucose uptake. *Physiol. Rev.* **93**, 993–1017 (2013).
56. Bjerregaard, P. et al. Inuit health in Greenland: a population survey of life style and disease in Greenland and among Inuit living in Denmark. *Int. J. Circumpolar Health* **62**, 3–79 (2003).
57. Ekblom-Bak, E., Björkman, F., Hellenius, M. L. & Ekblom, B. A new submaximal cycle ergometer test for prediction of VO2max. *Scand. J. Med. Sci. Sports* **24**, 319–326 (2014).
58. Wojtaszewski, J. F. P., Hansen, B. F., Kiens, B. & Richter, E. A. Insulin signaling in human skeletal muscle: time course and effect of exercise. *Diabetes* **46**, 1775–1781 (1997).
59. Kristensen, J. M., Treebak, J. T., Schjerling, P., Goodyear, L. & Wojtaszewski, J. F. P. Two weeks of metformin treatment induces AMPK-dependent enhancement of insulin-stimulated glucose uptake in mouse soleus muscle. *Am. J. Physiol. Endocrinol. Metab.* **306**, E1099–E1109 (2014).
60. Albers, P. H. et al. Human muscle fiber type-specific insulin signaling: Impact of obesity and type 2 diabetes. *Diabetes* **64**, 485–497 (2015).
61. Bornø, A., Foged, L. & Van Hall, G. Glucose and glycerol concentrations and their tracer enrichment measurements using liquid chromatography tandem mass spectrometry. *J. Mass Spectrom.* **49**, 980–988 (2014).
62. Seidemann, J., Lowry, O. H. & Passonneau, J. V. A flexible system of enzymatic analysis. Academic Press, New York, 1972. 291 S., 32 Abb., 15 Tab., Preis $ 14.00. *Starch (Stärke)* **25**, 322 (1973).
63. Højlund, K. et al. Dysregulation of glycogen synthase COOH- and NH_2-terminal phosphorylation by insulin in obesity and type 2 diabetes mellitus. *J. Clin. Endocrinol. Metab.* **94**, 4547–4556 (2009).
64. Rueden, C. T. et al. ImageJ2: ImageJ for the next generation of scientific image data. *BMC Bioinf.* **18**, 529 (2017).
65. Dobin, A. & Gingeras, T. R. Mapping RNA-seq reads with STAR. *Curr. Protoc. Bioinforma.* **51**, 11.14.1–11.14.19 (2015).
66. Wang, L. et al. Measure transcript integrity using RNA-seq data. *BMC Bioinf.* **17**, 58 (2016).
67. Graubert, A., Aguet, F., Ravi, A., Ardlie, K. G. & Getz, G. RNA-SeQC 2: efficient RNA-seq quality control and quantification for large cohorts. *Bioinformatics* **37**, 3048–3050 (2021).
68. Love, M. I., Huber, W. & Anders, S. Moderated estimation of fold change and dispersion for RNA-seq data with DESeq2. *Genome Biol.* **15**, 550 (2014).
69. Udeshi, N. D., Mertins, P., Svinkina, T. & Carr, S. A. Large-scale identification of ubiquitination sites by mass spectrometry. *Nat. Protoc.* **8**, 1950–1960 (2013).
70. Sinitcyn, P. et al. MaxDIA enables library-based and library-free data-independent acquisition proteomics. *Nat. Biotechnol.* **12**, 1563–1573 (2021).
71. Subramanian, A. et al. Gene set enrichment analysis: a knowledge-based approach for interpreting genome-wide expression profiles. *Proc. Natl Acad. Sci. USA* **102**, 15545–15550 (2005).
72. Mootha, V. K. et al. PGC-1α-responsive genes involved in oxidative phosphorylation are coordinately downregulated in human diabetes. *Nat. Genet.* **34**, 267–273 (2003).
73. Ritchie, M. E. et al. Limma powers differential expression analyses for fRNA-sequencing and microarray studies. *Nucleic Acids Res.* **43**, e47 (2015).
74. Benjamini, Y. & Hochberg, Y. Controlling the false discovery rate: a practical and powerful approach to multiple testing. *J. R. Stat. Soc. Ser. B* **57**, 289–300 (1995).
75. Ochoa, D. et al. An atlas of human kinase regulation. *Mol. Syst. Biol.* **12**, 888 (2016).
76. Abdul-Ghani, M. A., Molina-Carrion, M., Jani, R., Jenkinson, C. & DeFronzo, R. A. Adipocytes in subjects with impaired fasting glucose and impaired glucose tolerance are resistant to the anti-lipolytic effect of insulin. *Acta Diabetol.* **45**, 147–150 (2008).
77. Gutt, M. et al. Validation of the insulin sensitivity index (ISI0,120): comparison with other measures. *Diabetes Res. Clin. Pract.* **47**, 177–184 (2000).

Acknowledgements

We thank all Greenlandic Inuit that have participated in the study. We acknowledge the skilled technical help provided by B. Bolmgren and I.B. Nielsen (Department of Nutrition, Exercise and Sports, Faculty of Science, University of Copenhagen). We acknowledge K.A. Wickham (Department of Nutrition, Exercise and Sports, Faculty of Science, University of Copenhagen) for generating the graphical figure illustrations and L.L.S.S. Stevner (Department of Nutrition, Exercise and Sports, Faculty of Science, University of Copenhagen) for providing support on general data protection regulation. We thank P. Krustrup (University of Southern Denmark) for making the Inbody apparatus available for the study. We also thank K. Højlund (Steno Diabetes Center Odense and University of Southern Denmark) for valuable scientific and clinical insight and for helping with interpretation of data. We acknowledge the Core Facility for Integrated Microscopy, Faculty of Health and Medical Sciences, University of Copenhagen for skilled technical helped with the GLUT4 imaging analyses. Funding for the study was provided by research grants from Novo Nordisk Foundation (grant nos. NNF14OC0013057 to T.H. and NNF0070370 and NNF082659 to J.F.P.W.) and Steno Collaborative grants (grant nos. NNF17OC0028136 to M.E.J., T.H. and J.F.P.W.). Further funding for the study was provided by the Danish Council for Independent Research (grant nos. 8020-00288B to J.F.P.W. and 5053-00095B to J.M.K.) as well as the Danish Diabetes Academy, which is funded by the Novo Nordisk Foundation (grant no. NNF17SA0031406 to J.o.O. and R.K.). The Novo Nordisk Foundation Center for Basic Metabolic Research is supported by and unrestricted grant from the Novo Nordisk Foundation (grant no. NNF18CC0034900 to T.H.). D.E.J. is funded by an Australian Research Council Laureate Fellowship and B.H. was supported by a grant from the Danish Council for Independent

Research (grant no. 7016-00386B). None of the funding agencies had any role in the study design or in the collection and interpretation of data.

Author contributions

J.F.P.W., M.E.J., T.H. and J.M.K. designed the study. J.M.K. along with T.J.L., C.S.C., A.T., B.H., J. Onslev, J. Olesen, M.L.P., E.A.R. and J.F.P.W. did the recruitment, screening and initial clinical investigations of study participants in Nuuk. J.R.H., T.J.L., J.B.B., R.K., E.A.R., J.F.P.W. and J.M.K. performed the invasive clinical investigations in Copenhagen. J.B.B., D.E.S., J.R.K., N.S.H., J.F.H., A.G., S.E.S., B.H. and C.C.H. performed the biochemical analyses. C.F.R. and K.E.H. performed the RNA-seq and related bioinformatics analyses. E.J.N., S.J.H. and D.E.J. performed the proteomics analyses. T.E.J., Y.H., H.P. and N.G. contributed with scientific expertise. J.M.K., R.K. and J.F.P.W. wrote the first draft of the manuscript. All authors contributed to the interpretation of the results and the discussion as well as edited the manuscript. Finally all authors edited and revised the manuscript and approved the final version. J.M.K., R.K. and J.F.P.W. are the guarantors of this work and, as such, had full access to all the data in the study and take responsibility for the integrity of the data and the accuracy of the data analysis.

Competing interests

J.F.P.W. has ongoing collaborations with Pfizer Inc. and Novo Nordisk A/S unrelated to this study. M.E.J. has received research grants from AMGEN, AstraZeneca, Boehringer Ingelheim and Sanofi Aventis. M.E.J., B.H., J.R.H., D.E.S., J.M.K. and J.F.P.W. hold shares in Novo Nordisk A/S. J.M.K., J.R.H., J.F.H., D.E.K., K.E.H., N.G. and J.R.K. are currently employed by Novo Nordisk A/S. The other authors declare no competing interests.

Additional information

Extended data is available for this paper at https://doi.org/10.1038/s42255-024-01153-1.

Supplementary information The online version contains supplementary material available at https://doi.org/10.1038/s42255-024-01153-1.

Correspondence and requests for materials should be addressed to Jørgen F. P. Wojtaszewski.

Peer review information *Nature Metabolism* thanks Gregory Steinberg and the other, anonymous, reviewer(s) for their contribution to the peer review of this work. Primary Handling Editor: Ashley Castellanos-Jankiewicz, in collaboration with the *Nature Metabolism* team.

Reprints and permissions information is available at www.nature.com/reprints.

Publisher's note Springer Nature remains neutral with regard to jurisdictional claims in published maps and institutional affiliations.

Jonas M. Kristensen[1,13], Rasmus Kjøbsted[1,13], Trine J. Larsen[2], Christian S. Carl[1], Janne R. Hingst[1], Johan Onslev[1], Jesper B. Birk[1], Anette Thorup[1], Dorte E. Steenberg[1], Jonas R. Knudsen[1], Nicolai S. Henriksen[1], Elise J. Needham[3], Jens F. Halling[4], Anders Gudiksen[4], Carsten F. Rundsten[5], Kristian E. Hanghøj[6], Sara E. Stinson[5], Birgitte Hoier[7], Camilla C. Hansen[7], Thomas E. Jensen[1], Ylva Hellsten[7], Henriette Pilegaard[4], Niels Grarup[5], Jesper Olesen[8], Sean J. Humphrey[3], David E. James[3,9], Michael L. Pedersen[2,10], Erik A. Richter[1], Torben Hansen[5,14], Marit E. Jørgensen[2,11,12,14] & Jørgen F. P. Wojtaszewski[1,14]

[1]August Krogh Section for Molecular Physiology, Department of Nutrition, Exercise and Sports, Faculty of Science, University of Copenhagen, Copenhagen, Denmark. [2]Greenland Center of Health Research, Institute of Institute of Health and Nature, University of Greenland, Nuuk, Greenland. [3]Charles Perkins Centre, School of Life and Environmental Sciences, University of Sydney, Sydney, New South Wales, Australia. [4]Section for Cell Biology and Physiology, Department of Biology, University of Copenhagen, Copenhagen, Denmark. [5]Novo Nordisk Foundation Center for Basic Metabolic Research, Faculty of Health and Medical Sciences, University of Copenhagen, Copenhagen, Denmark. [6]The Bioinformatics Centre, Department of Biology, University of Copenhagen, Copenhagen, Denmark. [7]August Krogh Section for Human Physiology, Department of Nutrition, Exercise and Sports, Faculty of Science, University of Copenhagen, Copenhagen, Denmark. [8]Queen Ingrid Primary Health Care Center, Nuuk, Greenland. [9]Sydney Medical School, University of Sydney, Sydney, New South Wales, Australia. [10]Steno Diabetes Center Greenland, Nuuk, Greenland. [11]Steno Diabetes Center Copenhagen, Gentofte, Denmark. [12]National Institute of Public Health, University of Southern Denmark, Odense, Denmark. [13]These authors contributed equally: Jonas M. Kristensen, Rasmus Kjøbsted. [14]These authors jointly supervised this work: Torben Hansen, Marit E. Jørgensen, Jørgen F. P. Wojtaszewski. ✉e-mail: jw@nexs.ku.dk

https://doi.org/10.1038/s42255-024-01153-1

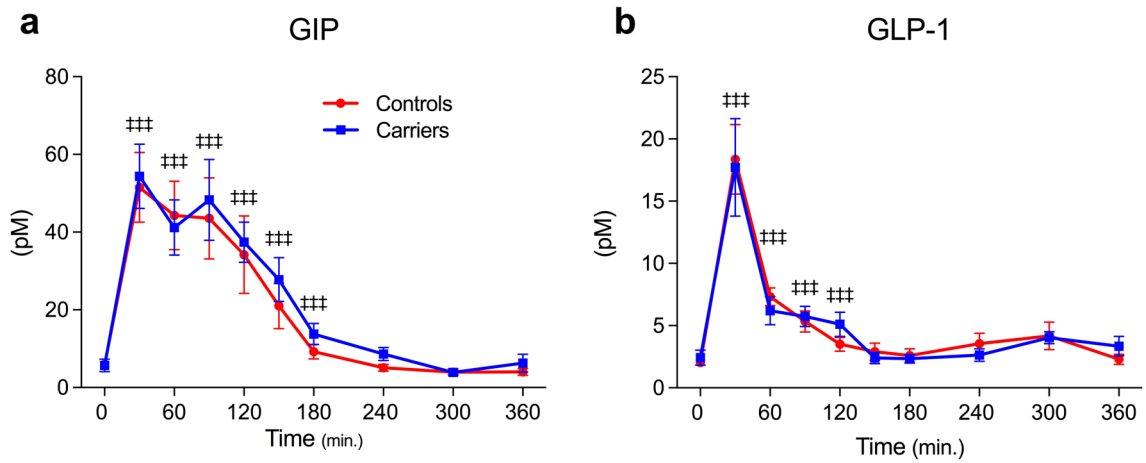

Extended Data Fig. 1 | Gut hormones during an extended oral glucose challenge in homozygous *TBC1D4* p.Arg684Ter variant carriers. **a**, **b**, Plasma levels of GIP (**a**) and GLP-1 (**b**) during an extended (6-h) oral glucose tolerance test (OGTT). ‡Different from basal (time = 0) in both groups. Three symbols = $P < 0.001$. $n = 8$ in Controls and $n = 7$ in TBC1D4 carriers. Data are means ± SEM. Data were analyzed using a two-way repeated ANOVA test (one factor repeated) and two-tailed Student–Newman-Keuls post hoc analyses for multiple comparisons.

https://doi.org/10.1038/s42255-024-01153-1

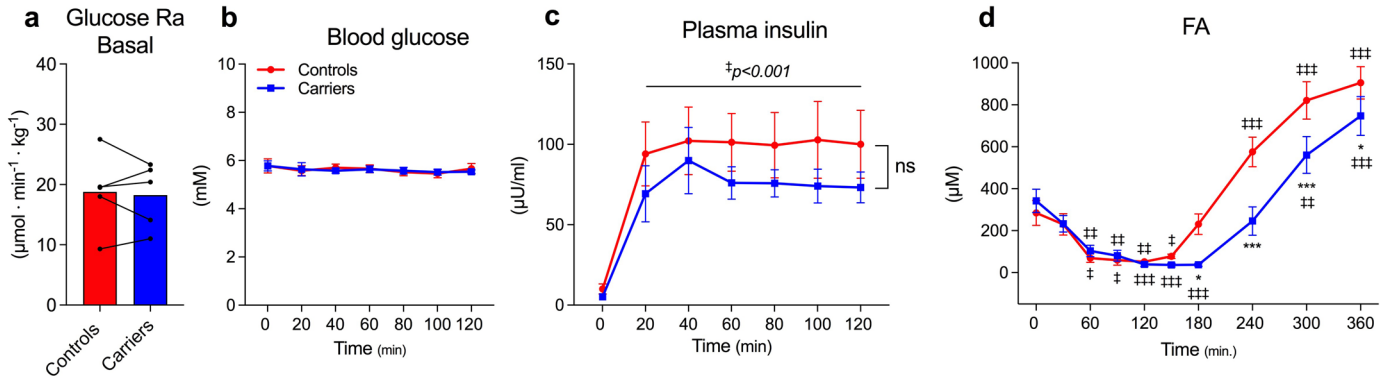

e

Gene Set	Size	ES	NES	NOM p-value	FDR q-value
TYPE I DIABETES MELLITUS	39	0,56	1,14	0,200	1,000
GLYCOLYSIS GLUCONEOGENESIS	58	0,54	1,13	0,180	1,000
STARCH AND SUCROSE METABOLISM	36	0,54	1,10	0,278	1,000
KEGG ADIPOCYTOKINE SIGNALING PATHWAY	65	0,51	1,07	0,297	1,000
KEGG TYPE II DIABETES MELLITUS	44	0,50	1,04	0,402	1,000
KEGG INSULIN SIGNALING PATHWAY	132	0,42	0,90	0,841	1,000
KEGG REGULATION OF ACTIN CYTOSKELETON	203	0,41	0,90	0,898	1,000
KEGG TOLL LIKE RECEPTOR SIGNALING PATHWAY	93	0,41	0,88	0,825	1,000
KEGG BIOSYNTHESIS OF UNSATURATED FATTY ACIDS	22	0,43	0,85	0,763	1,000
KEGG CITRATE CYCLE TCA CYCLE	30	0,40	0,81	0,866	1,000
KEGG OXIDATIVE PHOSPHORYLATION	125	0,35	0,76	0,988	1,000
KEGG FATTY ACID METABOLISM	42	0,31	0,63	0,987	0,994

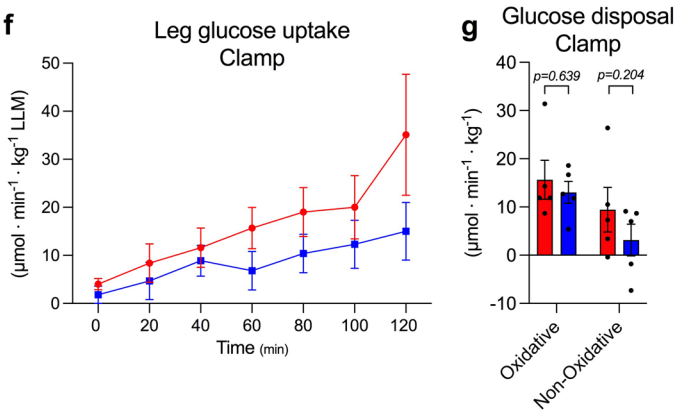

Extended Data Fig. 2 | Glycemic markers, oxidative and non-oxidative glucose disposal as well as adipose tissue GSEA during euglycemic-hyperinsulinemic clamp conditions in homozygous *TBC1D4* p.Arg684Ter variant carriers. a, Basal (Pre-clamp) endogenous glucose rate of appearance (Ra). **b**, **c**, Blood glucose levels (**b**) and plasma insulin concentrations (**c**) during the insulin clamp. **d**, Plasma fatty acids during an extended (6-h) oral glucose tolerance test (OGTT). **e**, RNA Gene Set Enrichment Analysis (GSEA) in adipose tissue obtained at the end of the insulin clamp with number of genes included in the gene set indicated by 'Size', Enrichment Score indicated by 'ES', Normalized Enrichment Score indicated by 'NES', Nominal P Value indicated by 'NOM p-value' and False Discovery Rate indicated by 'FDR q-value'. **f**, Leg glucose uptake during the 120 min insulin clamp. **g**, Glucose disappearance rate displayed as oxidative and non-oxidative glucose metabolism during the insulin clamp steady state period (90 min). ‡Different from basal (time = 0) in both groups (line indicates main effect). *Difference between TBC1D4 carriers and Controls. One symbol = $P < 0.05$, two symbols = $P < 0.01$ and three symbols = $P < 0.001$. $n = 5$ in both groups (**a**–**c**, **f**, **g**) and $n = 8$ in Controls and $n = 7$ in TBC1D4 carriers (**d**). Data are means ± SEM. Data were analyzed using a two-tailed paired students t-test (**a**, **g**) as well as a two-way repeated ANOVA test (one factor repeated (**d**) and two factor repeated (**b**, **c**)) and two-tailed Student-Newman-Keuls post hoc analyses for multiple comparisons (**b**–**d**). Statistical analyses were not applied to data in panel **f**. LLM, leg lean mass. AU, arbitrary units.

https://doi.org/10.1038/s42255-024-01153-1

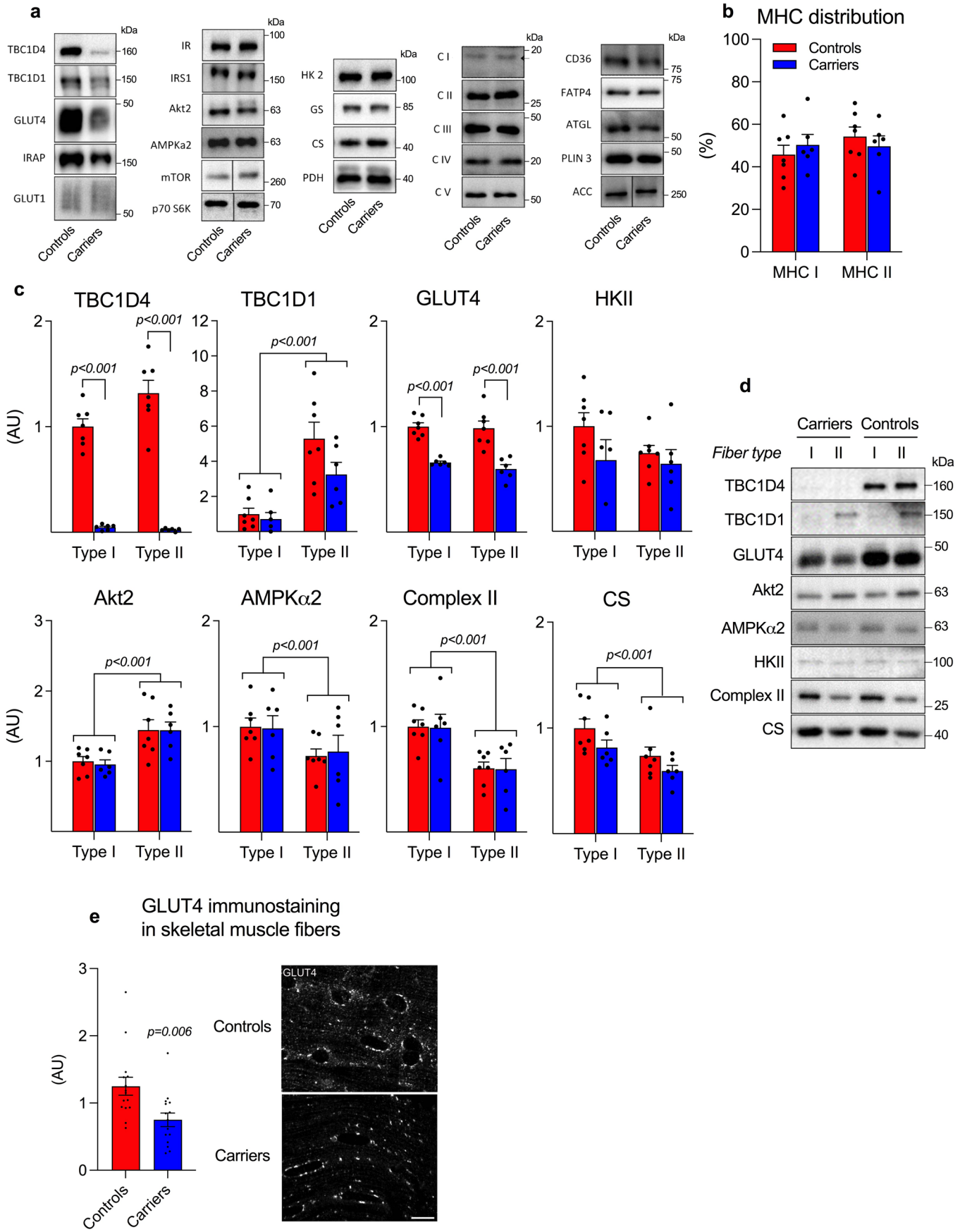

Extended Data Fig. 3 | See next page for caption.

https://doi.org/10.1038/s42255-024-01153-1

Extended Data Fig. 3 | Muscle fiber type-specific protein content and GLUT4 immunostaining in muscle fibers from homozygous *TBC1D4* p.Arg684Ter variant carriers. a, Representative immunoblots for data related to figure panel 2 h. **b**, **c**, Distribution of Myosin Heavy Chains (MHC) (**b**) and regulatory metabolic (**c**) proteins in MHC-defined type 1 and type 2 skeletal muscle fiber bundles. **d**, Representative immunoblots. **e**, Quantification of GLUT4 imaging by confocal microscopy of isolated skeletal muscle fibers. $n = 7$ in Controls and $n = 6$ in TBC1D4 carriers (**b**, **c**). $n = 15$ fibers obtained from 3 subjects (4 to 6 fibers/subject) in each group (**e**). Data are means ± SEM. Data were analyzed using a two-tailed non-paired students t-test (**e**) as well as a two-way repeated ANOVA test (one factor repeated) and two-tailed Student-Newman-Keuls post hoc analyses for multiple comparisons (**b**, **c**). AU, arbitrary units. Scale bar in panel **e** is 10 μm.

https://doi.org/10.1038/s42255-024-01153-1

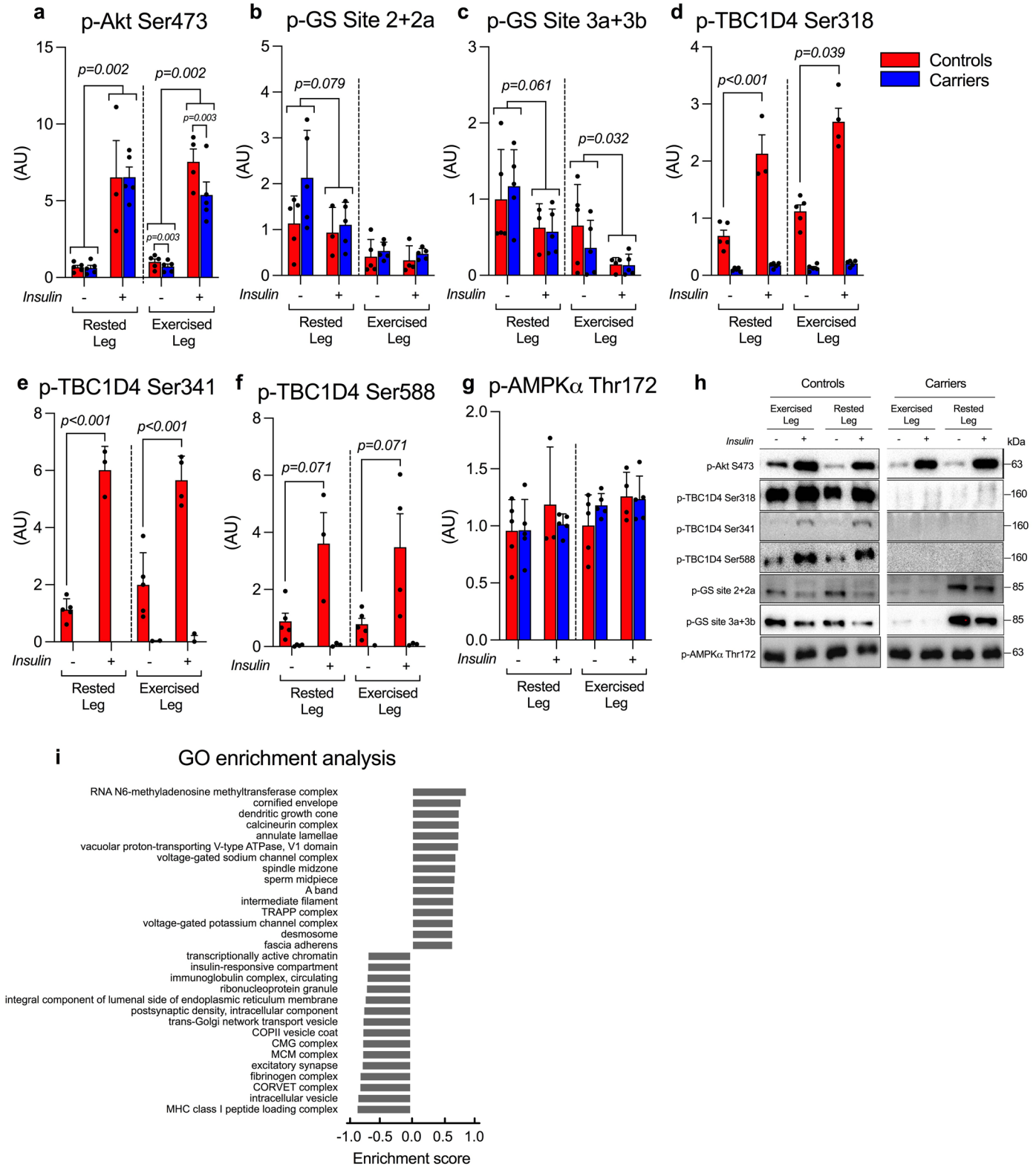

Extended Data Fig. 4 | Insulin- and AMPK-related signaling is not compromised in skeletal muscle from homozygous *TBC1D4* p.Arg684Ter variant carriers after a single bout of exercise. a–**g**, Skeletal muscle protein phosphorylation of Akt Ser473 (**a**), GS site 2 + 2a (Ser7 + Ser10) (**b**), GS site 3a + 3b (Ser640 + Ser644) (**c**), TBC1D4 Ser318 (**d**), TBC1D4 Ser341 (**e**), TBC1D4 Ser588 (**f**) and AMPKα Thr172 (**g**) in rested and prior exercised muscle before and at the end of the insulin clamp. **h**, Representative immunoblots. **i**, The top 15 up- and downregulated Gene Ontology (GO) pathways of the proteome. $n = 5$ (Rested and Exercised leg – insulin), $n = 3$ (Rested leg + insulin), and $n = 4$ (Exercised leg + insulin) in Controls and $n = 5$ in TBC1D4 carriers (**a**–**g**). The difference in n is due to missing biopsies as well as depleted sample material. $n = 5$ (**i**). Data are means ± SEM. Data were analyzed using a two-way repeated ANOVA test (two factor repeated) and two-tailed Student-Newman-Keuls post hoc analyses for multiple comparisons (**a**–**g**). AU, arbitrary units. LLM, leg lean mass.

https://doi.org/10.1038/s42255-024-01153-1

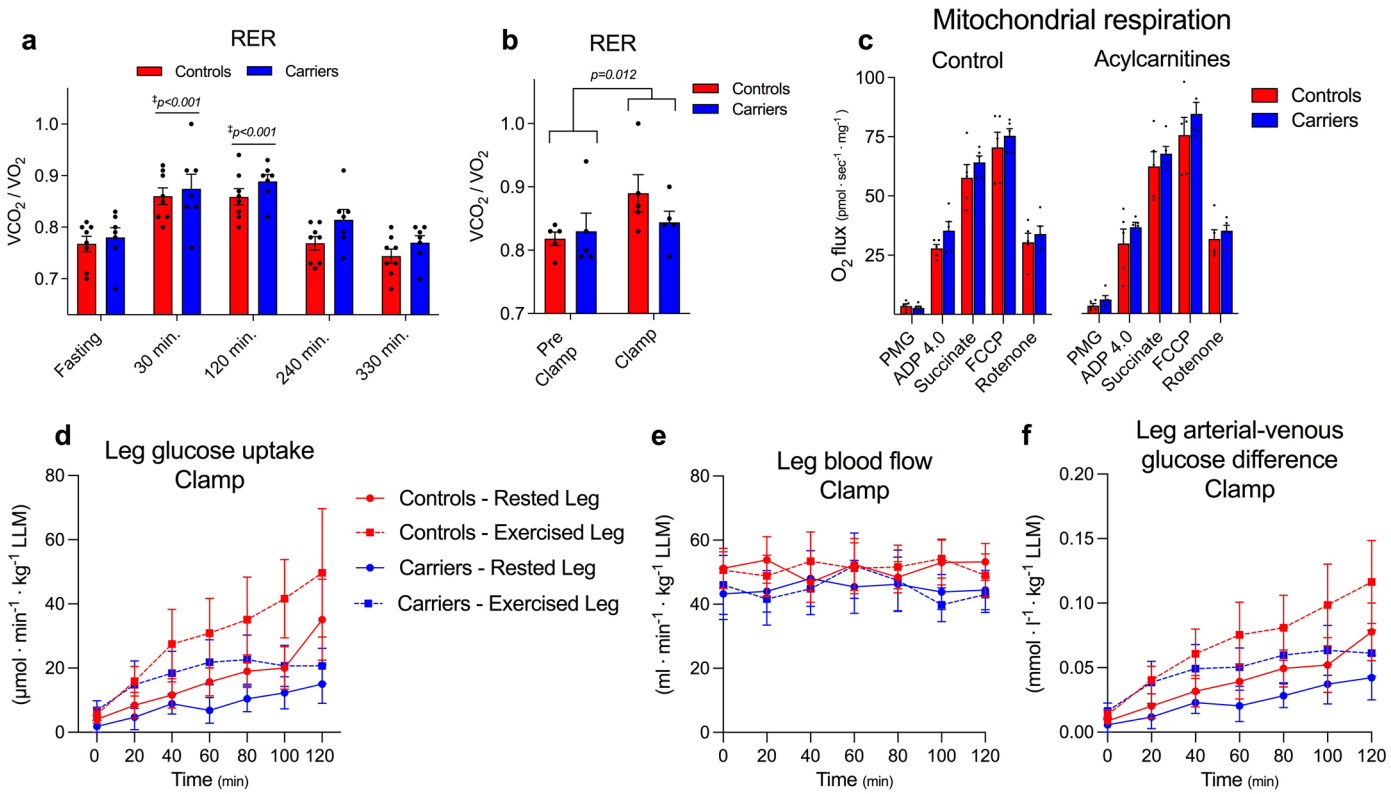

Extended Data Fig. 5 | Leg glucose uptake, blood flow and arterial-venous glucose difference during euglycemic-hyperinsulinemic clamp conditions as well as whole-body substrate utilization and mitochondrial respiration in permeabilized muscle fibers from homozygous *TBC1D4* p.Arg684Ter variant carriers. a, **b**, Respiratory Exchange Ratio (RER) during an extended (6-h) oral glucose tolerance test (OGTT) (**a**) as well as before and at the end of the insulin clamp (**b**). **c**, Mitochondrial respiration rate (O_2 flux) in permeabilized muscle fibers in the presence or absence of acylcarnitines (palmitoylcarnitine/octanoylcarnitine). **d**–**f**, Glucose uptake (**d**), blood flow (**e**) and arterial-venous glucose difference (**f**) in the prior rested and exercised leg during the 120 min insulin clamp. ‡Different from fasting in both groups. $n = 5$ in both groups (**b**–**e**) and $n = 8$ in Controls and $n = 7$ in TBC1D4 carriers (**a**). Data are means ± SEM. Data were analyzed using a two-way repeated ANOVA test (one factor repeated (**a**) and two factor repeated (**b**–**e**)) and two-tailed Student-Newman-Keuls post hoc analyses for multiple comparisons (**a**–**e**). LLM, leg lean mass.

https://doi.org/10.1038/s42255-024-01153-1

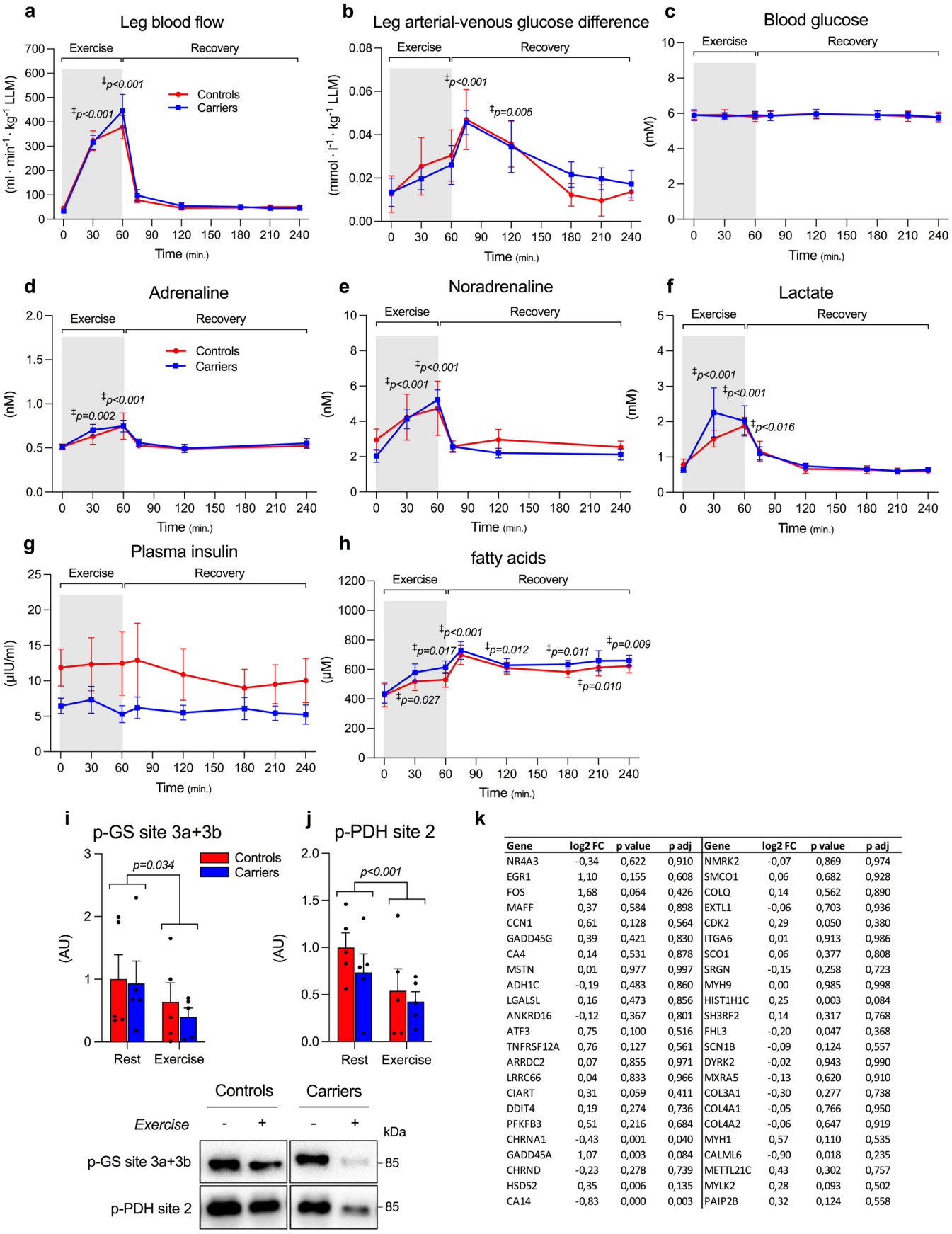

k

Gene	log2 FC	p value	p adj	Gene	log2 FC	p value	p adj
NR4A3	-0,34	0,622	0,910	NMRK2	-0,07	0,869	0,974
EGR1	1,10	0,155	0,608	SMCO1	0,06	0,682	0,928
FOS	1,68	0,064	0,426	COLQ	0,14	0,562	0,890
MAFF	0,37	0,584	0,898	EXTL1	-0,06	0,703	0,936
CCN1	0,61	0,128	0,564	CDK2	0,29	0,050	0,380
GADD45G	0,39	0,421	0,830	ITGA6	0,01	0,913	0,986
CA4	0,14	0,531	0,878	SCO1	0,06	0,377	0,808
MSTN	0,01	0,977	0,997	SRGN	-0,15	0,258	0,723
ADH1C	-0,19	0,483	0,860	MYH9	0,00	0,985	0,998
LGALSL	0,16	0,473	0,856	HIST1H1C	0,25	0,003	0,084
ANKRD16	-0,12	0,367	0,801	SH3RF2	0,14	0,317	0,768
ATF3	0,75	0,100	0,516	FHL3	-0,20	0,047	0,368
TNFRSF12A	0,76	0,127	0,561	SCN1B	-0,09	0,124	0,557
ARRDC2	0,07	0,855	0,971	DYRK2	-0,02	0,943	0,990
LRRC66	0,04	0,833	0,966	MXRA5	-0,13	0,620	0,910
CIART	0,31	0,059	0,411	COL3A1	-0,30	0,277	0,738
DDIT4	0,19	0,274	0,736	COL4A1	-0,05	0,766	0,950
PFKFB3	0,51	0,216	0,684	COL4A2	-0,06	0,647	0,919
CHRNA1	-0,43	0,001	0,040	MYH1	0,57	0,110	0,535
GADD45A	1,07	0,003	0,084	CALML6	-0,90	0,018	0,235
CHRND	-0,23	0,278	0,739	METTL21C	0,43	0,302	0,757
HSD52	0,35	0,006	0,135	MYLK2	0,28	0,093	0,502
CA14	-0,83	0,000	0,003	PAIP2B	0,32	0,124	0,558

Extended Data Fig. 6 | See next page for caption.

https://doi.org/10.1038/s42255-024-01153-1

Extended Data Fig. 6 | Leg blood flow, leg arterial-venous glucose difference, blood glucose, plasma hormones and skeletal muscle genes are regulated similarly in Controls and homozygous *TBC1D4* p.Arg684Ter variant carriers during and in recovery from exercise. a, **b**, Leg blood flow (**a**) and leg arterial-venous glucose difference during 1 h of knee-extensor exercise and 3 h recovery. **c**–**h**, Concentrations of blood glucose (**c**), plasma adrenaline (**d**), plasma noradrenaline (**e**), blood lactate (**f**), plasma insulin (**g**) and plasma fatty acids (**h**) before, during and 3 h into recovery from exercise. **i**, **j**, Skeletal muscle protein phosphorylation of glycogen synthase (GS) site 3a + 3b (**i**) and pyruvate dehydrogenase (PDH) site 2 (Ser300) (**j**) in the previously rested leg (Rest) as well as immediately after exercise in the exercised leg (Exercise). Representative immunoblots are shown below the data panels. **k**, Regulation of selected skeletal muscle genes 3 h into recovery from exercise in Controls and TBC1D4 carriers. The selected genes have previously been reported top exercise responsive with acute aerobic exercise (see ref. 46 in main article). The selected genes are indicated by "Gene", while the Log2 Fold Changes of the exercise response between Controls and TBC1D4 carriers are indicated by "Log2 FC". Positive values indicate a higher exercise response in TBC1D4 carriers than in Controls, while negative values indicate a lower exercise response in TBC1D4 carriers than in Controls. The nominal p values are indicated by "p value", while the adjusted p values used to correct for multiple testing are indicated by "p adj". ‡Different from Rest (time=0) within both groups. n = 5 in Controls and in TBC1D4 carriers. Data are means ± SEM. Data were analyzed using a two-way repeated ANOVA test (two factor repeated: time/group and genotype) and two-tailed Student-Newman-Keuls post hoc analyses for multiple comparisons. AU, arbitrary units.

https://doi.org/10.1038/s42255-024-01153-1

Extended Data Table 1 | Clinical characteristics

Characteristics	Controls (n=8)	TBC1D4 carriers (n=8)
Age (years)	54 ± 3	56 ± 3
Biological sex (Female/Male)	4/4	4/4
BMI ($kg\ m^{-2}$)	29 ± 2	28 ± 2
Weight (kg)	82 ± 8	76 ± 6
Body fat content (%)	32 ± 2	35 ± 3
Body muscle mass (kg)	30 ± 3	28 ± 3
EU-admixture (%)	27 ± 5	18 ± 6
$VO_{2\ peak}$ ($ml\ O_2\ min^{-1}$)#	2107 ± 232	1819 ± 149
Fitness level ($ml\ O_2\ kg^{-1}\ min^{-1}$)#	25 ± 2	24 ± 2
Fitness level ($ml\ O_2\ kg\ lean\ mass^{-1}\ min^{-1}$)	67 ± 3	65 ± 5
Fasting plasma insulin (pM)	63 ± 19	45 ± 3
Fasting blood glucose (mM)	5.8 ± 0.2	5.7 ± 2
HOMA-IR ($mM * mU\ L^{-1}$)	2.72 ± 0.91	1.85 ± 0.18
HbA1c (%)	5.4 ± 0.1	6.1 ± 0.2**
2-hour blood glucose (mM)##	6.5 ± 0.6	10.9 ± 0.9***
2-hour plasma insulin (pM)##	296 ± 145	482 ± 110*
$ISI_{0,120}$##	5.1 ± 0.8	2.8 ± 0.4*
FA (µM)##	285 ± 59	342 ± 55
TG (mM)##	0.98 ± 0.16	0.92 ± 0.16
Glycerol (µM)##	18 ± 5	14 ± 5
HDL cholesterol (mM)##	1.35 ± 0.05	1.54 ± 0.09(*)
LDL cholesterol (mM)##	3.83 ± 0.16	3.81 ± 0.42
Total Cholesterol (mM)##	5.50 ± 0.19	5.64 ± 0.52
Adipose-IR##	25 ± 9	19 ± 2

Data represent means±SEM. BMI, Body mass index. $VO_{2\ peak}$, maximum rate of oxygen consumption. HOMA-IR, Homeostatic Model Assessment for Insulin Resistance. HbA1c, hemoglobin A1c. ISI, Insulin Sensitivity Index. FA, fatty acids. TG, triacylglycerol. HDL, high density lipoprotein. LDL, low density lipoprotein. Adipose-IR: Adipose tissue Insulin-Resistance index. Data were analyzed using an unpaired t-test. (*)P=0.077; *P<0.05; **P<0.01; ***P<0.001 Difference between Controls and TBC1D4 carriers. #; n=6 in Controls and n=6 in TBC1D4 carriers. ##; n=7 in TBC1D4 carriers.

https://doi.org/10.1038/s42255-024-01153-1

Extended Data Table 2 | Clinical characteristics of subjects participating in the experimental day in Denmark

Characteristics	Controls (n=5)	TBC1D4 carriers (n=5)
Age (years)	54 ± 3	55 ± 4
Biological sex (Female/Male)	2/3	2/3
BMI (kg m^{-2})	30 ± 2	29 ± 2
Weight (kg)	86 ± 12	82 ± 8
Body fat content (%)	32 ± 3	31 ± 4
Body muscle mass (kg)	32 ± 4	31 ± 3
EU-admixture (%)	28 ± 8	27 ± 5
$VO_{2\ peak}$ (ml O_2 min^{-1})	2145 ± 280	1885 ± 180
Fitness level (ml O_2 kg^{-1} min^{-1})	25 ± 2	23 ± 2
Fitness level (ml O_2 kg lean $mass^{-1}$ min^{-1})	67 ± 3	62 ± 6
Fasting blood glucose (mM)	5.8 ± 0.3	5.8 ± 0.3
HbA1c (%)	5.4 ± 0.1	6.0 ± 0.2*
2-hour blood glucose (mM)#	6.9 ± 0.8	10.5 ± 1.5(*)

Data represent means±SEM. BMI, Body mass index. $VO_{2\ peak}$, maximum rate of oxygen consumption. HbA1c, hemoglobin A1c. Data were analyzed using a paired t-test except for data on '2-h blood glucose' that were analyzed using an unpaired t-test due to a missing value in the TBC1D4 carriers. *P<0.05 and (*)P=0.058; Different from Controls. #; n=4 in TBC1D4 carriers.

nature portfolio

Corresponding author(s): Jørgen F.P. Wojtaszewski

Last updated by author(s): Aug 29, 2024

Reporting Summary

Nature Portfolio wishes to improve the reproducibility of the work that we publish. This form provides structure for consistency and transparency in reporting. For further information on Nature Portfolio policies, see our Editorial Policies and the Editorial Policy Checklist.

Statistics

For all statistical analyses, confirm that the following items are present in the figure legend, table legend, main text, or Methods section.

n/a	Confirmed	
☐	☒	The exact sample size (*n*) for each experimental group/condition, given as a discrete number and unit of measurement
☐	☒	A statement on whether measurements were taken from distinct samples or whether the same sample was measured repeatedly
☒	☐	The statistical test(s) used AND whether they are one- or two-sided *Only common tests should be described solely by name; describe more complex techniques in the Methods section.*
☒	☐	A description of all covariates tested
☐	☒	A description of any assumptions or corrections, such as tests of normality and adjustment for multiple comparisons
☐	☒	A full description of the statistical parameters including central tendency (e.g. means) or other basic estimates (e.g. regression coefficient) AND variation (e.g. standard deviation) or associated estimates of uncertainty (e.g. confidence intervals)
☐	☒	For null hypothesis testing, the test statistic (e.g. *F*, *t*, *r*) with confidence intervals, effect sizes, degrees of freedom and *P* value noted *Give P values as exact values whenever suitable.*
☒	☐	For Bayesian analysis, information on the choice of priors and Markov chain Monte Carlo settings
☒	☐	For hierarchical and complex designs, identification of the appropriate level for tests and full reporting of outcomes
☒	☐	Estimates of effect sizes (e.g. Cohen's *d*, Pearson's *r*), indicating how they were calculated

Our web collection on statistics for biologists contains articles on many of the points above.

Software and code

Policy information about availability of computer code

Data collection	SentrySuite software (v.3.20.8), Lunar Prodigy Advance Encore software (v.16), BioRad Image Lab (v.6.0.1), Oroboros Datlab (v.7.0), Zeiss Zen Black 2012, RNA-SeQC2 (v.2.3.4), DESeq2 (v.1.28.1).
Data analysis	Microsoft Excel 2016, Fuji ImageJ (v.2.7.0), BioRad Image Lab (v.6.0.1), GraphPad Prism (v.9.0), SigmaPlot (v.14.0), MaxQuant (v2.1.3.0), FastQC (v.0.11.9), Gencode (v.34), STAR (v.2.7.9a), GSEA tool (v.4.3.2), KEGG database gene set (v.2023.1), Uniprot Reference database (May 2021), R programming (v.3.6.2 and v.4.0.2) including LIMMA and ksea R packages.

For manuscripts utilizing custom algorithms or software that are central to the research but not yet described in published literature, software must be made available to editors and reviewers. We strongly encourage code deposition in a community repository (e.g. GitHub). See the Nature Portfolio guidelines for submitting code & software for further information.

Data

Policy information about availability of data

All manuscripts must include a data availability statement. This statement should provide the following information, where applicable:

- Accession codes, unique identifiers, or web links for publicly available datasets
- A description of any restrictions on data availability
- For clinical datasets or third party data, please ensure that the statement adheres to our policy

RAW data and processed output tables have been deposited in the PRIDE proteomeXchange repository and can be accessed at https://www.ebi.ac.uk/pride/ with

the accession PXD045301, username: reviewer_pxd045301@ebi.ac.uk and password: HFFgPBlT. Raw RNA-sequencing reads produced in this work have been deposited to the EGA database, accession number EGAD50000000059. All other data that support the findings of this study are available from the corresponding author upon reasonable request.

Research involving human participants, their data, or biological material

Policy information about studies with human participants or human data. See also policy information about sex, gender (identity/presentation), and sexual orientation and race, ethnicity and racism.

Reporting on sex and gender	Sex of the study participants was reported by self-identification. Both males and females study participants were recruited in the study with a similar proportion. Due to the low sample size in our data, we found it inappropriate to disaggregate our data for sex.
Reporting on race, ethnicity, or other socially relevant groupings	All study participants originated from the Greenlandic Inuit population and had an European genetic admixture of ~25-30%.
Population characteristics	We investigated a total of 16 study participants. Clinical characteristics of the study participants can be found in the Extended Data Table 1 and 2 of the manuscript.
Recruitment	All study participants were recruited from the Greenlandic cohort register called the Inuit Health in Transition (IHIT). Due to the low accessibility of the homozygous TBC1D4 variant carriers, all homozygous carriers who voluntary signed up, met the inclusion criteria and gave informed consent to participate were included in the study. Control subjects were recruited to the study to individually match the TBC1D4 variant carriers, according to age, self-reported sex, European genetic admixture, BMI and physical fitness. Inclusion criteria were: females and males, 25-70 years of age, BMI 20-35 kg/m2, no medical treatment for type 2 diabetes. Study participants were provided with financial compensation for their involvement in the research to offset any expenses incurred and to acknowledge their contribution to the study.
Ethics oversight	All study participants were provided oral and written study information. Written informed consent was obtained from all study participants before entering the study. The study was approved by the Commission for Scientific Research in Greenland and the Copenhagen Ethics Committee in Denmark as well as conformed to the declaration of Helsinki.

Note that full information on the approval of the study protocol must also be provided in the manuscript.

Field-specific reporting

Please select the one below that is the best fit for your research. If you are not sure, read the appropriate sections before making your selection.

☒ Life sciences ☐ Behavioural & social sciences ☐ Ecological, evolutionary & environmental sciences

For a reference copy of the document with all sections, see nature.com/documents/nr-reporting-summary-flat.pdf

Life sciences study design

All studies must disclose on these points even when the disclosure is negative.

Sample size	No statistical methods were used to predetermine sample size. Sample size (number of study participants) were determined by the available number of study participants carrying the TBC1D4 variant.
Data exclusions	No data were excluded from the analyses.
Replication	Replication of the study results were not performed due to the strained logistics of recruiting and testing the study participants.
Randomization	N/A - all participants underwent the same experimental procedure.
Blinding	The investigators were not blinded to the group allocation (TBC1D4 variant vs. Control) because all study participants were genotyped before entering the study. Part of the data collection were performed blinded including blood analyses of hormones, enzyme activities, mitochondrial respirometry, GLUT4 imaging, RNA-sequencing and proteomics while other parts of the data collection were performed non-blinded including immunoblotting analyses. Investigators were blinded during data analysis but not blinded during the statistical analyses.

Reporting for specific materials, systems and methods

We require information from authors about some types of materials, experimental systems and methods used in many studies. Here, indicate whether each material, system or method listed is relevant to your study. If you are not sure if a list item applies to your research, read the appropriate section before selecting a response.

Materials & experimental systems

n/a	Involved in the study
☐	☒ Antibodies
☒	☐ Eukaryotic cell lines
☒	☐ Palaeontology and archaeology
☒	☐ Animals and other organisms
☐	☒ Clinical data
☒	☐ Dual use research of concern
☒	☐ Plants

Methods

n/a	Involved in the study
☒	☐ ChIP-seq
☒	☐ Flow cytometry
☒	☐ MRI-based neuroimaging

Antibodies

Antibodies used

The following primary antibodies are listed with supplier name, catalog number, clone name / lot number, and dilution in that order (N/A, not applicable):
TBC1D4, Abcam, ab189890, GR320789-2, 0.5 µg/ml
TBC1D1, Proteintech, 22124-1-AP, N/A, 1:1000
TBC1D1, Abcam, ab229504, GR3248015-2, 1 µg/ml
GLUT4, Thermo Fisher, PA1-1065, SB242399, 1:1000
GLUT4, Thermo Fisher, PA5-23052, WJ3403509, 1:100
IRAP, Custom-made by prof. Susanne R. Keller, N/A, N/A, 1 µg/ml
GLUT1, Millipore, 07-1401, 3481410, 1 µg/ml
IR, Custom-made by prof. Ken Siddle, CT-21, N/A, 1:1000
IRS1, Upstate Biotechnology, 06-248, 31556, 0.75 µg/ml
Akt2, CST, 3063, 4, 1:1000
AMPKα2, SCBT, sc-19131, C0116, 0.2 µg/ml
mTOR, CST, 2972, 6, 1:250
p70 S6 kinase, CST, 9202, 20, 1:1000
HK2, SCBT, sc-130358, J3017, 1 µg/ml
GS, Custom-made by prof. Oluf Pedersen, N/A, N/A, 1:40000
CS, Abcam, ab96600, N/A, 1:1000
PDH E1α, Custom-made by prof. D.G. Hardie and prof. Henriette Pilegaard, N/A, N/A, 1 µg/ml
OXPHOS Complex 1, Abcam, ab110411, J5383, 1:10000
OXPHOS Complex 2, Abcam, ab110411, J5383, 1:10000
OXPHOS Complex 3, Abcam, ab110411, J5383, 1:10000
OXPHOS Complex 4, Abcam, ab110411, J5383, 1:10000
OXPHOS Complex 5, Abcam, ab110411, J5383, 1:10000
CD36, R&D Systems, AF2519, VYQOZ15041, 1:1000
FATP4, Abcam, ab200353, GR3267173-2, 1:1000
ATGL, CST, 2138, 4, 1:1000
Perilipin 3, Proscience Incorporated, 3881, N/A, 1:500
ACC, Jackson ImmunoResearch Labs, 016-030-084, 108001, 1:2000
p-Akt T308, CST, 9275, N/A, 1:1000
p-Akt S473, CST, 9271, 12, 1:1000
p-p70 S6K T389, CST, 9205, 21+22, 1:2000
p-TBC1D4 S318, CST, 8619, 1, 1:1000
p-TBC1D4 S341, Custom-made by prof. D.G. Hardie and prof. Carol MacKintosh, N/A, N/A, 4 µg/ml
p-TBC1D4 S588, CST, 8730, 1, 1:1000
p-TBC1D4 T642 (T649), CST, 8881, 3, 1:1000
p-TBC1D1 S596 (S590), CST, 6927, N/A, 1:1000
p-TBC1D4 S704 (S711), Custom-made by associate prof. Jonas T. Treebak, N/A, N/A, 1 µg/ml
p-GS site 2+2a, Custom-made by prof. D.G. Hardie and prof. Jørgen Wojtaszewski, N/A, N/A, 1.5 µg/ml
p-GS site 3a+3b, Custom-made by prof. D.G. Hardie and prof. Jørgen Wojtaszewski, N/A, N/A, 1 µg/ml
p-AMPKα T172, CST, 2531, 1b, 1:1000
p-ACC S221 (S212), CST, 3661, 10, 1:1000
p-P38 T180/Y182, CST, 9211, 23, 1:1000
p-TBC1D1 S237 (S231), Millipore, 07-2268, 2952313, 1:1000
p-PDH site 1, Custom-made by prof. D.G. Hardie and prof. Henriette Pilegaard, N/A, N/A, 1 µg/ml
p-PDH site 2, Custom-made by prof. D.G. Hardie and prof. Henriette Pilegaard, N/A, N/A, 1 µg/ml

The following secondary antibodies are listed with supplier name, catalog number, and dilution:
Goat-anti-rabbit-IgG-HRP, Jackson ImmunoResearch Labs, 111-035-045, 1:5000
Goat-anti-mouse-IgG-HRP, Jackson ImmunoResearch Labs, 115-035-062, 1:5000
Rabbit-anti-goat-IgG-HRP, Jackson ImmunoResearch Labs, 305-035-003, 1:5000
Rabbit-anti-sheep-IgG-HRP, Jackson ImmunoResearch Labs, 313-035-003, 1:5000

Validation

Some antibodies have previously been validated in KO cells/tissue. Other antibodies were validated by the manufacturer and confirmed with western blotting by their expected molecular weight or in OE/KO cells and tissue.
TBC1D4: validated (human) in the current study by Western blotting using muscle biopsy samples from homozygous TBC1D4 variant carriers that do not express TBC1D4 protein in skeletal muscle.

TBC1D1 (Proteintech): https://www.ptglab.com/products/TBC1D1-Antibody-22124-1-AP.htm
TBC1D1 (Abcam): https://www.abcam.com/en-dk/products/primary-antibodies/tbc1d1-antibody-ab229504
GLUT4: https://www.thermofisher.com/antibody/product/GLUT4-Antibody-Polyclonal/PA1-1065
GLUT4: https://www.thermofisher.com/antibody/product/GLUT4-Antibody-Polyclonal/PA5-23052
IRAP: validated in PMID: 8621739
GLUT1: https://www.merckmillipore.com/DK/en/product/Anti-GLUT-1-Antibody-CT,MM_NF-07-1401?bd=1
IR: https://absoluteantibody.com/product/anti-hinsr-c-terminus-ir-ct-21/
IRS1: https://www.emdmillipore.com/US/en/product/Anti-IRS1-Antibody,MM_NF-06-248
Akt2: https://www.cellsignal.com/products/primary-antibodies/akt2-d6g4-rabbit-mab/3063
AMPKα2: Validated in PMID: 31010958
mTOR: https://www.cellsignal.com/products/primary-antibodies/mtor-antibody/2972
p70 S6 kinase: https://www.cellsignal.com/products/primary-antibodies/p70-s6-kinase-antibody/9202
HK2: https://www.scbt.com/p/hxk-ii-antibody-1a7
GS: Validated in PMID: 17928598
CS: https://www.abcam.com/en-dk/products/primary-antibodies/citrate-synthetase-antibody-ab96600#
PDH E1α: validated in PMID: 17957032
OXPHOS Complex 1: https://www.abcam.com/en-dk/products/panels/total-oxphos-human-wb-antibody-cocktail-ab110411
OXPHOS Complex 2: https://www.abcam.com/en-dk/products/panels/total-oxphos-human-wb-antibody-cocktail-ab110411
OXPHOS Complex 3: https://www.abcam.com/en-dk/products/panels/total-oxphos-human-wb-antibody-cocktail-ab110411
OXPHOS Complex 4: https://www.abcam.com/en-dk/products/panels/total-oxphos-human-wb-antibody-cocktail-ab110411
OXPHOS Complex 5: https://www.abcam.com/en-dk/products/panels/total-oxphos-human-wb-antibody-cocktail-ab110411
CD36: https://www.rndsystems.com/products/mouse-cd36-sr-b3-antibody_af2519
FATP4: https://www.abcam.com/en-dk/products/primary-antibodies/slc27a4-fatp4-antibody-epr17319-26-ab200353
ATGL: https://www.cellsignal.com/products/primary-antibodies/atgl-antibody/2138
Perilipin 3: https://www.prosci-inc.com/product/tip47-antibody-3881/
p-Akt T308: https://www.cellsignal.com/products/primary-antibodies/phospho-akt-thr308-antibody/9275
p-Akt S473: validated in PMID: 31444134
p-p70 S6K T389: https://www.cellsignal.com/products/primary-antibodies/phospho-p70-s6-kinase-thr389-antibody/9205
p-TBC1D4 S318: validated (human) in the current study by Western blotting using muscle biopsy samples from homozygous TBC1D4 variant carriers that do not express TBC1D4 protein in skeletal muscle.
p-TBC1D4 S341: validated (human) in the current study by Western blotting using muscle biopsy samples from homozygous TBC1D4 variant carriers that do not express TBC1D4 protein in skeletal muscle.
p-TBC1D4 S588: validated (human) in the current study by Western blotting using muscle biopsy samples from homozygous TBC1D4 variant carriers that do not express TBC1D4 protein in skeletal muscle.
p-TBC1D4 T642 (T649): validated (human) in the current study by Western blotting using muscle biopsy samples from homozygous TBC1D4 variant carriers that do not express TBC1D4 protein in skeletal muscle.
p-TBC1D1 S596 (S590): https://www.cellsignal.com/product/productDetail.jsp?productId=6927
p-TBC1D4 S704 (S711): Validated in PMID: 37074686
p-GS site 2+2a: validated in PMID: 1983
p-GS site 3a+3b: validated in PMID: 32504885
p-AMPKα T172: validated in PMID: 32504885
p-ACC S221 (S212): validated in PMID: 24185692
p-P38 T180/Y182: https://www.cellsignal.com/products/primary-antibodies/phospho-p38-mapk-thr180-tyr182-antibody/9211
p-TBC1D1 S237 (S231): Validated in PMID: 31010958
p-PDH site 1: validated in PMID: 17957032
p-PDH site 2: validated in PMID: 17957032

Clinical data

Policy information about clinical studies

All manuscripts should comply with the ICMJE guidelines for publication of clinical research and a completed CONSORT checklist must be included with all submissions.

Clinical trial registration	NCT04170972
Study protocol	The study protocol is provided with the article
Data collection	Pre-screening and clinical tests in Greenland were conducted at a clinical laboratory at Queen Ingrid's Hospital in Nuuk from November 2017 to August 2018. The main experimental test was performed at the Department of Nutrition, Exercise and Sports in Copenhagen, Denmark from May 2018 to February 2019.
Outcomes	Primary and secondary outcome measures have been thoroughly pre-defined in the clinical trial registration. The primary outcome measures include changes in leg glucose uptake and whole-body insulin sensitivity that have been assessed during a hyperinsulinemic-euglycemic clamp (gold-standard). Also, global unbiased transcriptomic (RNA-sequencing) and proteomic (Mass spectrometry) muscle analyses as well as the molecular signaling signature (immonoblotting) of skeletal muscle following exercise and insulin stimulation were part of the primary outcome measures.

Plants

Seed stocks	N/A
Novel plant genotypes	N/A
Authentication	N/A